Immersion cooling effect of dielectric liquid and self-rewetting fluid on smooth and porous surface

Pin Chen, Souad Harmand, Safouene Ouenzerfi

Immersion Cooling Effect of Dielectric Liquid and Self-rewetting Fluid on Smooth and Porous Surface

Pin Chen, Souad Harmand, Safouene Ouenzerfi*

Laboratoire d'Automatique, de Mécanique et d'Informatique Industrielles et Humaines (LAMIH-UMR CNRS 8201), Université Polytechnique Hauts-de-France, Valenciennes 59313, France

ABSTRACT

Dielectric liquid Novec 7300 and 5% 1-butanol aqueous solution are applied for immersion cooling of heater in order to investigate effect of nucleate boiling and self-rewetting on heat transfer. Experimental results are compared with water as common liquid for immersion cooling. In first part of study, bare heater is heated until temperature arrives at certain levels (from 100 °C to 500 °C), and then immersed in liquid for observing rapid cooling performance of these three solutions. In 5% 1-butanol binary solution, heater temperature decreases the fastest and stabilizes at the lowest level. Inversed thermal Marangoni flow induced by vertical temperature difference along heat surface is supposed to assist vapor bubbles separation and improve convective heat dissipation. From 200 °C, vapor film appears on the surface of heater immersed in Novec 7300 and water, whose thickness is dependent of surface temperature but independent of heat flux. In second part of study, immersion cooling performances of three testing liquids on heater with or without porous shells of different porosity are explored with increasing heating power. At different heat flux input, shell porosity, capillary effect, inverse thermal Marangoni effect and pool boiling stages influence heat transfer efficiency of each fluid-heater combination. A curve of optimal heat transfer coefficient is established, which is beneficial for selection of suitable fluid-heater combination.

Keywords: immersion cooling; dielectric liquid; thermal Marangoni effect; nucleate boiling; capillary effect.

Nomenclature

A heat transfer surface area [cm^2]

a pore diameter [m]

C heat capacity [J/kg·K]

e vapor film thickness [mm]

h_{cv} convective heat transfer coefficient [$W/m^2 \cdot K$]

I current [I]

k thermal conductivity [W/m·K]

L characteristic length [m]

Ma_T thermal Marangoni number [-]

q heat flux [W/cm^2]

R thermal resistance [$m^2 \cdot K/W$]

T temperature [°C]

U voltage [V]

Greek symbols

α thermal diffusivity [m^2/s]

ε emissivity [-]

σ Stefan-Boltzmann constant [$J/s \cdot m^2 \cdot k^4$]

γ interfacial tension [mN/m]

μ dynamic viscosity [mPa·s]

θ contact angle [°]

ΔT temperature difference between heater and environmental liquid [K]

ΔT_{int} temperature difference across interface [K]

ΔT_{ws} wall superheat [K]

Δp capillary pressure [Pa]

Subscript

air air

c heating cartridge

cv convection

env environment

l liquid

r radiation

s solid shell

sat saturation

st stabilization

tot total

w wall

1. Introduction

In recent decades, the semiconductor industry is experiencing very rapid growth. Integrated circuits design undergoes the trend of miniaturization and increased transistors density, which brings the challenge of high heat flux dissipation. Heat transfer problem will limit the essential demand in high processing speed and abnormal temperature could increase failure probability and reduce service life of electronic component. Liquid immersion cooling is considered as one of efficient and potential heat dissipation solution due to high specific heat and nucleate boiling of cooling liquid.

Heat transfer of immersion cooling can be divided in several stages with increasing heat flux through electronic component gradually. Starting with low surface temperature, heat transfer mode is only naturel convection. With further increase of heater surface superheat, discrete bubbles are generated at nucleation sites like cavities and scratches on solid surface. The number of active nucleation sites increases with rise of heat flux and correspondingly more bubbles gather to form coalescence on heater surface until total coverage. At this moment, film boiling occurs. Before incipience of film boiling, the highest heat flux is called critical heat flux (CHF). At transition boiling stage, increase of surface temperature superheat degrades heat flux instead. Accumulation of more and more vapor slugs on heater surface deteriorates heat transfer and most electronic element cannot stand so high superheat. Thus the operation temperature of electronic device should be below this superheat value in order to prevent the arrival of critical heat flux.

The object of improving liquid immersion cooling is to increase critical heat flux and meanwhile decrease surface temperature superheat. Numerous experimental researches are concentrated on two approaches: appropriate cooling liquid and surface modification.

In recent years, dielectric liquid is considered as a potential liquid for high heat flux immersion cooling with advantages of low dielectric constant and chemical inertness. In the study of Arik and Bar-Cohen[1], application of perfluorocarbon liquids for immersion cooling of microelectronic device can attain dissipated heat flux of 20 W/cm^2 at atmospheric conditions. Heat transfer coefficient achieved was approximately three times as the one of forced air convection. Then they obtained pool boiling CHF of 53 W/cm^2 and 59 W/cm^2 for Novec dielectric liquids HFE-7100 and HFE-7200 at elevated environmental pressure of 3 bars respectively[2]. However, due to relative high saturation pressure, low thermal conductivity and low specific heat, incipience of nucleate boiling is advanced for dielectric liquid and its CHF is lower than common cooling liquid. In order to delay incipience of nucleate boiling and enhance CHF of dielectric liquid, liquid subcooling[3, 4], surface inclination[4], dissolved gas[3, 5] and dielectric binary mixture[6, 7] attract greatly attention of thermodynamic researchers. Another potential liquid for immersion cooling is self-rewetting fluids with the most important advantage as inverse Marangoni effect. Since all the liquids trend to flow from low surface tension region to high surface tension region, temperature or component concentration gradient on interface will generate surface tension gradient as well as so-called Marangoni flow[8]. Unlike ordinary liquids, some high-carbon alcohol dilute aqueous solutions were found to display an abnormal surface tension increase with temperature growth from a specific value, which are termed as self-rewetting fluids[9]. Thus self-rewetting fluid streams

towards hotter place within specific temperature gradient range, whose direction is opposite to ordinary Marangoni flow. Application of self-rewetting fluids has been proved to enhance heat transfer performance in liquid evaporation[10, 11], spray cooling[12], heat pipes[13-15], microchannel[16] and pool boiling[17-20]. Hu et al.[17] tested nucleate pool boiling on horizontal heated wire with water, 5 wt% ethanol aqueous solution and 5 wt% butanol aqueous solution. Both binary solutions demonstrate enhanced CHF than water due to Marangoni effect induced convection. However CHF of 5 wt% butanol aqueous solution is the highest because of intense inverse solutal Marangoni flow, which has the same direction as thermal Marangoni flow. Sakashita et al.[20] investigated saturated pool boiling performance of 2-propanol aqueous mixtures with variation of alcohol concentration. They found that the mixtures of 3.0 to 4.7 mol% 2-propanol concentration reveal the highest CHF which is 1.7 times of testing with water. Combination of thermal and solutal Marangoni flow induced by temperature and concentration gradient of micro liquid layer under bubbles was considered as explanation reason for enhanced CHF of self-rewetting fluids. Despite of numerous promising experimental results, the mechanism of heat transfer performance improvement by application of self-rewetting fluids has not yet been fully understood.

On the other hand, surface modification methods can be classified in macroscale (finned surface[21], porous mesh[22], porous foam[23, 24]), microscale (surface roughening[25], patterning micro-fins[26, 27], porous microstructure coating[28], micro-channels with reentrant cavities[29], dendritic porous microstructures[30], micro-dimpled surface[31], graphite coating[32]) and nanoscale (nanoparticles[33, 34], nanoporous[35] and nano film coating[36], nanofluid induced nanoparticles deposition[37]) surface enhancement techniques

for pool boiling. Moreover various hybrid techniques (macro enhanced surface with microstuds[38] and microporous coating[39], microfins[40] and microchannels[41] with nanostructures, hybrid wettability surface[42]) are applied to improve heat transfer coefficient and critical heat flux. Most experimental results revealed augmentation of heat transfer coefficient and critical heat flux of pool boiling. However there are still some controversial conclusions. Liu et al.[22] succeeded in improving nucleate boiling heat transfer coefficient of methanol and HFE-7100 with porous mesh layer at low wall superheat (ΔT_{ws} < 10 K). However both heat transfer coefficient and critical heat flux were deteriorated at high wall superheat (ΔT_{ws} > 10 K). Kim et al.[27] applied micro-finned surface to enhance pool boiling heat transfer and critical heat flux of deionized water and they found that if the gap size between pin-fins exceeds the critical value of 10-20 μm, heat transfer performance will be deteriorated. Jun et al.[33] investigated increased pool boiling heat transfer coefficient of water and ethanol on copper nanofibers covered surface in comparison with plain surface, but there is no observation of critical heat flux enhancement. Chang and You[28] utilized hybrid method comprised of microfins and microporous coating in order to improve nucleate boiling of FC-87 and R-123. They found that heat transfer coefficient and critical heat flux are higher than the case of uncoated surface at heat flux below 5 W/cm^2. But when heat flux exceeds 10 W/cm^2, both thermal characteristics are lower than plain surface. The enhanced surface technique has various limits in pool boiling performance improvement, thus fully understanding of heat transfer mechanism is contributing to the design of efficient heat removal system.

In this study, the combination of dielectric liquid, self-rewetting fluid and porous metallic foam was investigated in pool boiling performance. The experimental results were compared with water and plain heat exchange surface. The comparison of properties for water and Novec 7300 are listed in Table 1. Figure 1 presents surface tension of three testing liquids (water, 5% 1-butanol binary solution and Novec 7300). Despite of high dielectric strength, Novec 7300 is chemically inert to metal. Although its thermal properties are lower than water, its lower surface tension and higher volatility are supposed to increase wetting area, evaporation rate and then heat transfer performance. The other candidate liquid is water-1-butanol mixture solution. Because Novec 7300 is insoluble with water or 1-butanol, the self-rewetting fluid is made from 95 wt% water and 5 wt% 1-butanol. Obviously surface tension of 5% 1-butanol binary solution shows upward trend when temperature exceeds around 50 °C, which is so-called self-rewetting characteristic. Effects of capillary force, Marangoni flow and metallic foam porosity in heat dissipation of electronic component are the focus of experimental observations.

	Dielectric Strength (MV/m)	Viscosity (mPa·s)	Saturated vapor pressure (kPa)	Specific heat (J/kg·K)	Heat of vaporization (kJ/kg)	Thermal conductivity (W/m·K)	Boiling point (°C)
Water	65 - 70	1.00	2.3	4184	2260	0.592	100
Novec 7300	> 98	1.18	5.9	1140	102	0.063	98 [43]

Table 1 Properties of water and Novec 7300

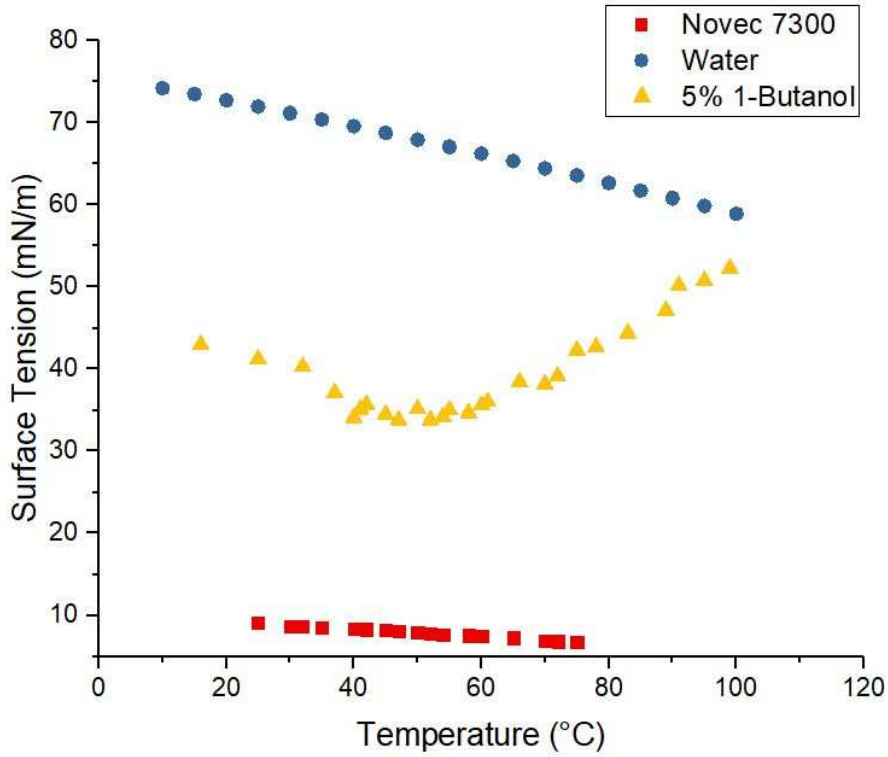

Figure 1 Surface tension of water, 5% 1-butanol binary solution and Novec 7300 as a function of temperature.

2. Experiment setup and procedures

Sometimes electronic element will exceed working temperature with occasional overload. Thus the increased heat flux needs to be dissipated by effective cooling method and the abnormal temperature requires to be reduced to ordinary range rapidly. In the section of rapid cooling, 5% 1-butanol binary solution and Novec 7300 dielectric liquid were tested for rapid cooling performance as working fluid and then experimental results were compared with the case of pure water which is the common working fluid for heat dissipation. The tests are preliminary, so the dissipated heat flux q is relative low from 0.4 W/cm^2 to 2.3 W/cm^2. Figure 2(a) presents experimental setup. A heating

cartridge Vulstar® (Reference 20264-15 with integrated thermocouple type K, l = 40 mm, Ø = 8mm) was used as heat source, which was connected to an electronic controller. The maximum power that heating cartridge can attain is 250 W. Three testing solutions were filled in a transparent vessel with open top. A microscopic camera (KEYENCE VW-600C, resolution 640 x 480) was applied to investigate boiling condition on heater surface. Heater was heated to arrive at certain temperatures in the air and then it was immediately immersed into testing solution to investigate the rapid cooling performance. The position of heater is fixed for each test, the distance between top of heater and liquid free surface is about 1cm. The integrated thermocouple of heater was connected to a Graphtec midi LOGGER to record temperature variation during immersion cooling. The experiment was carried out at environmental condition and cooling process is fast, thus the temperature of testing solution stays at around 20 °C which was measured by a supplementary thermocouple type K.

In the section of immersion cooling, heat transfer performances of three solutions were tested at higher heating power where heat flux can attain around 25 W/cm^2. Heater was completely immersed in testing solution during experiments at ambient condition. Different heating power was applied for 5 minutes in order to wait for stabilization of heater temperature. Heater is heated so long in testing solution that the increase of environmental liquid temperature is no longer negligible. A cooler was utilized to maintain environmental liquid temperature, whose serpentine tube surrounds heater (Figure 2(b)). The refrigerant circulates in serpentine tube and the operation temperature is from -10 °C to 100 °C. A thermocouple was placed between serpentine tube and heater in order to measure and control liquid bulk temperature. In the past decade,

numerous researches demonstrated that application of porous surface in immersion cooling can increase heat transfer coefficient and critical heat flux, and reduce surface temperature of electronic component. Thus, in the second section of experiments, two porous shells (P1 and P2) were fabricated from copper foam of different porosity. The porosity of P2 is higher than P1. Also a flat brass shell was made for comparing heat transfer enhancement with porous shells (Figure 3). Their physical and thermodynamic properties are listed in Table 2. The advantage of porous media is that capillary force will lead cooling liquid toward heater surface. The aim is to accelerate separation of bubbles from heating surface during nucleate boiling stage and reduce thickness of vapor film during film boiling stage. Thereby thermal resistance caused by vapor will be decreased and correspondingly cooling performance will be improved. Moreover the increased heat exchange area and high effective thermal conductivity will simultaneously enhance heat transfer coefficient.

No matter which experiment section, each test was repeated for three times for different fluid-heater combination and different heating power. The nominal uncertainty of K-type thermocouple is ±0.75 % and the bulk temperature of liquid is controlled within ±1 °C. According to the method of Morrat[44], the uncertainties of heat flux and heat transfer coefficient are estimated as 0.52 % and 1.11-8.93 %, respectively.

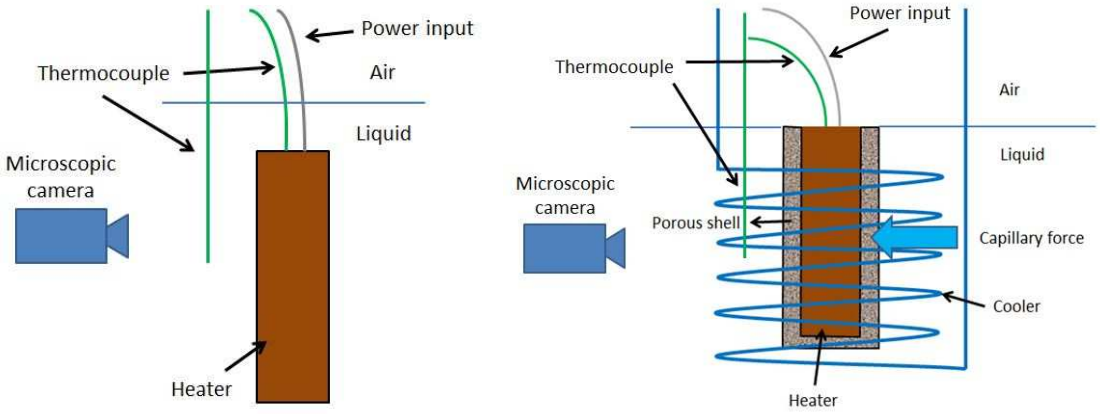

(a) Rapid cooling (b) Immersion cooling

Figure 2 Schema of experimental setup.

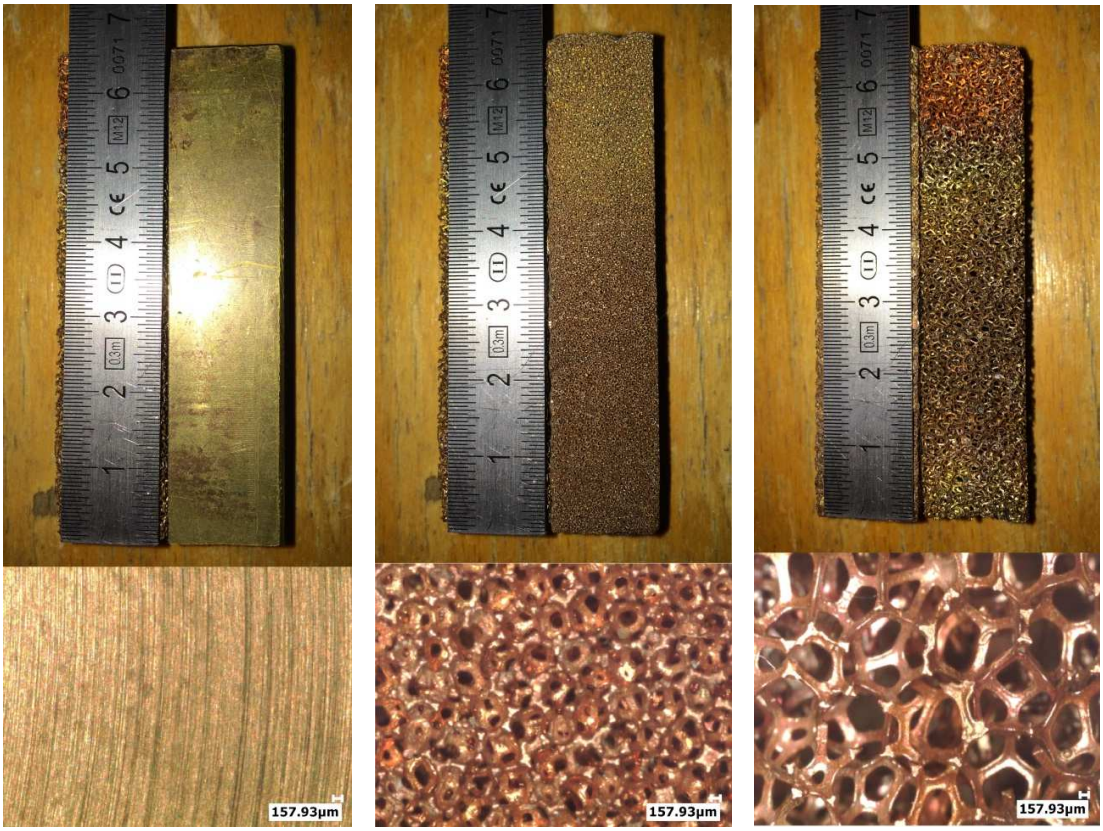

P0 P1 P2

Figure 3 Two porous copper foam shells of different porosity (P1 and P2) and a flat brass shell (P0) and microscopic structure images of three shells.

Shell Type	Average Pore Diameter (mm)	Porosity (%)	Permeability (m^2)	Effective Thermal Conductivity (W/m·K)
P0	0	0	0	125
P1	0.423	90	7.24×10^{-8}	39.61
P2	0.635	96	1.238×10^{-6}	16.24

Table 2 Physical and thermodynamic properties of three shells.

3. Results and discussion

3.1 Rapid cooling

In this section, the case of 1.7 W/cm^2 heat flux will be illustrated as an example. With this heat flux input, the increase of heater's temperature will follow the red heating curve in Figure 4 and the maximum can attain about 500 °C in the air. When temperature arrives at test value (T_c = 100 °C, 200 °C, 300 °C, 400 °C or 500 °C), heater will be immediately plunged into test solution (water, 5% 1-butanol binary solution or Novec 7300). After immersion in liquid, heater temperature decreases quickly at the beginning and finally stays stable at certain level. This stabilized temperature is dependent on solution type and heating power, but initial surface temperature before dipping in liquid does not show evident effect on stabilized temperature.

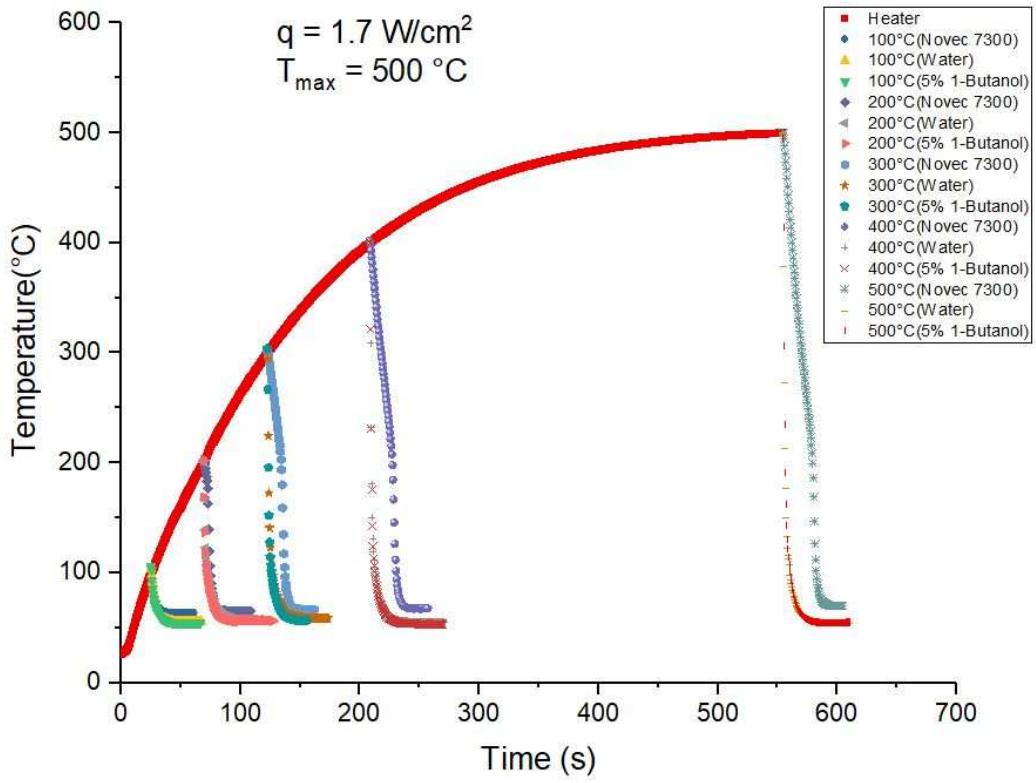

Figure 4 Temperature evolution of heater in the air and in testing solutions as a function of time.

The microscopic images of heater at the moment when immersed in liquid are shown in Figure 5. Because of high saturated vapor pressure, Novec 7300 is more volatile than two other solutions. According to microscope investigation, the vapor film appears on heater surface at the beginning when heater temperature T_c exceeds 200 °C. Film boiling lasts for a considerable long period (5s ~ 25s) and vapor film duration increases with initial heater surface temperature before immersion. When T_c reduces to around 180 °C, film boiling begins to transform to nucleate boiling from two ends of heater towards middle section. For water, film boiling can be investigated also from T_c = 200 °C and vapor film duration is relative short (1s ~ 10s). For 5% 1-butanol binary solution, only at

higher surface temperature T_c = 400 °C or 500 °C, vapor film can last for very short period (1s ~ 2S). To explain this evident difference of vapor film duration, one reason is that the saturated pressure of 5% 1-butnaol solution is the lowest among these solutions; the other reason is that when heater is dipped into liquid, the lower end is cooled firstly. Consequently a significant temperature gradient lies on heater surface. The self-rewetting characteristic of 1-butanol aqueous solution generates the inverse Marangoni flow which flows from colder region (lower end) towards hotter region (up end), thus vapor film or bubbles can be removed swiftly. The diameter of heater is 7.962 mm. By taking advantage of microscopic images, the external diameter with vapor film of heater can be measured by integrated software in microscope and vapor film thickness is the half value of external diameter minus heater diameter. The results are presented in Figure 6. Vapor film thickness increases with rise of heater temperature for each solution. The case of Novec 7300 shows the thickest vapor film while 5% 1-butanol solution displays the thinnest one. By means of comparison with different heating power, vapor film thickness does not demonstrate obvious relationship with heat flux. Vapor film thickness depends on heater surface temperature.

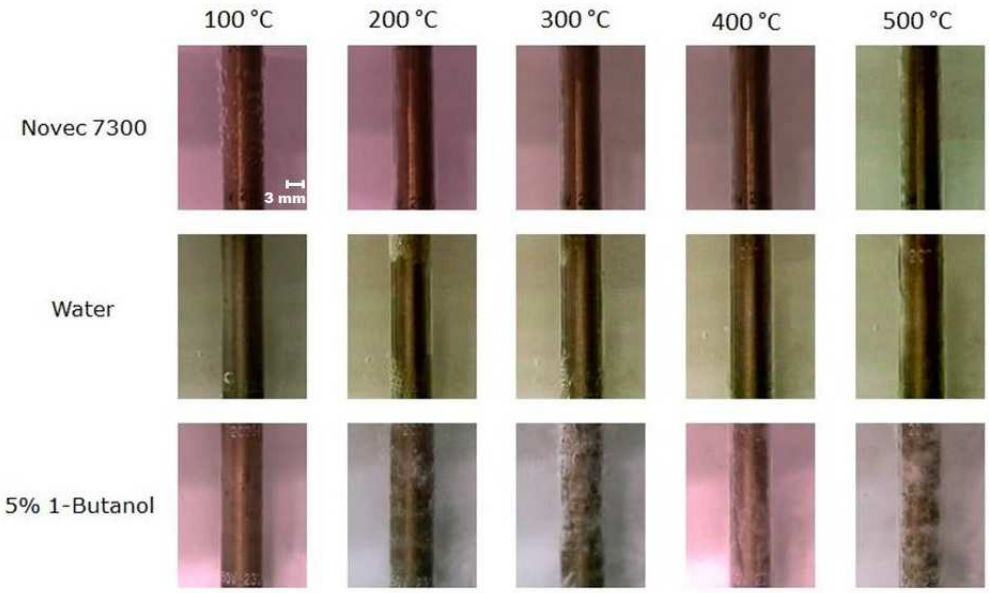

Figure 5 Microscopic images of heater at initial moment when immersed in liquid.

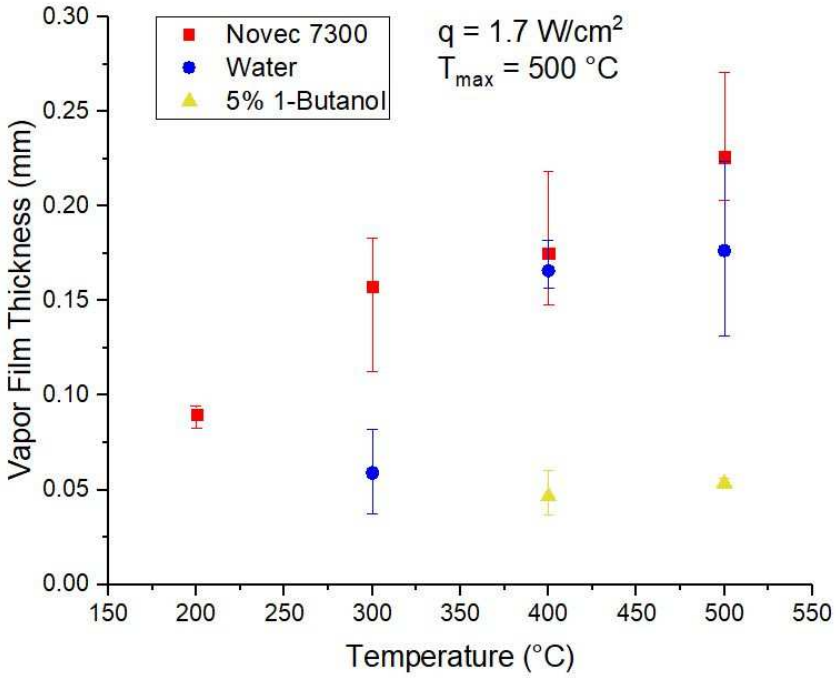

Figure 6 Vapor film thicknesses as a function of heater surface temperature before immersion.

Figure 7 represents the evolution of heater temperature immersed in three solutions. For the case of T_c = 100 °C, heater temperature development in every liquid follows the solution of Newton's law of cooling:

$$T(t) = T_{env} + (T(0) - T_{env})e^{-t/r} \quad (1)$$

where T_{env} is the environment temperature, $T(0)$ is the initial temperature of object, $r=hA/C$, h is the heat transfer coefficient, A is the heat transfer surface area, C is heat capacity of object. Heater temperature decreases quickly after dipped in each liquid and then the temperature cooling rate reduces with the decline of temperature different between heater and cooling liquid. Finally heater temperature stabilizes at a certain level. The stabilized temperature in 5% 1-butanol binary solution is the lowest and the temperature decline rate is the highest among three testing liquids. It is explained by that the specific heat of 1-butanol is higher than others liquids. Another more important reason is the reverse Marangoni effect generated by temperature gradient, which conducts 1-butanol binary solution to wet heater surface. The colder conducted liquid not only reduces heater surface temperature but also enhances naturel convection. Refer to five temperature tests the stabilized temperature of heater is independent of initial heater temperature, but increases with augmentation of heat flux. As mentioned above, vapor film boiling appears in Novec 7300 from T_c = 200 °C. Accordingly temperature evolution of heater in Novec 7300 is divided in two stages: 1. linear reduction during vapor film boiling, 2. exponential decay when vapor film boiling disappears. Thermal conduction is dominant in vapor film boiling and temperature reduction rate is much lower than other solutions due to low thermal conductivity of Novec 7300 vapor and lack of thermal convection assistance. Therefore this segmented cooling has potential

application for sensitive electronic element. Abrupt temperature reduction will produce important impact on some sensitive electronic element. Via immersion in dielectric liquid, temperature of electronic element will decrease moderately to a relative low level and then will be rapidly cooled to working temperature range in order to avoid the damage by thermal stress impact. By choosing dielectric liquid (vapor saturated pressure, boiling point, thermal conductivity etc.) or surface materiel of different characteristics, appropriate temperature reduction rate for stage 1 and suitable critical temperature where vapor film boiling disappears can be obtained for the cooling of specific electronic element.

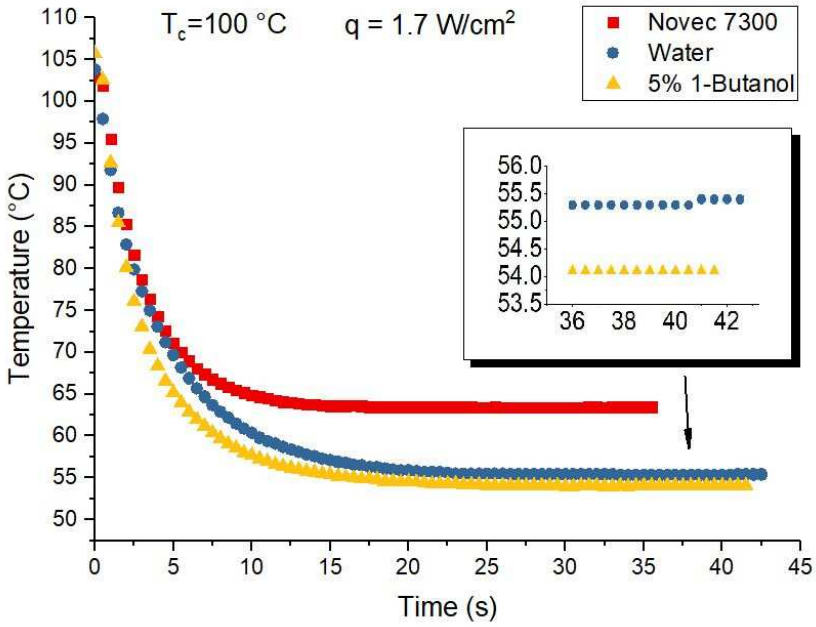

(a)

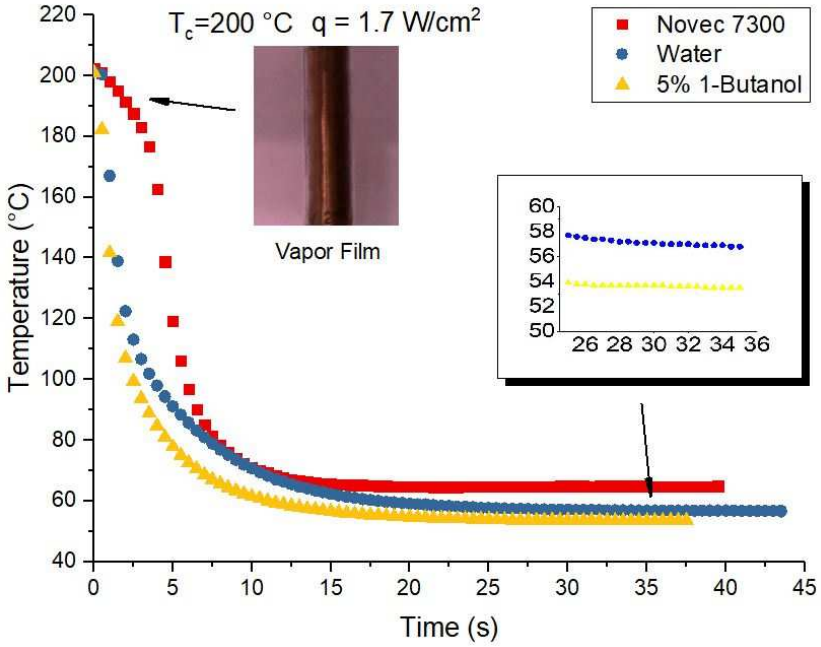
T$_c$=200 °C q = 1.7 W/cm^2
Novec 7300
Water
5% 1-Butanol
Vapor Film
Temperature (°C)
Time (s)

(b)

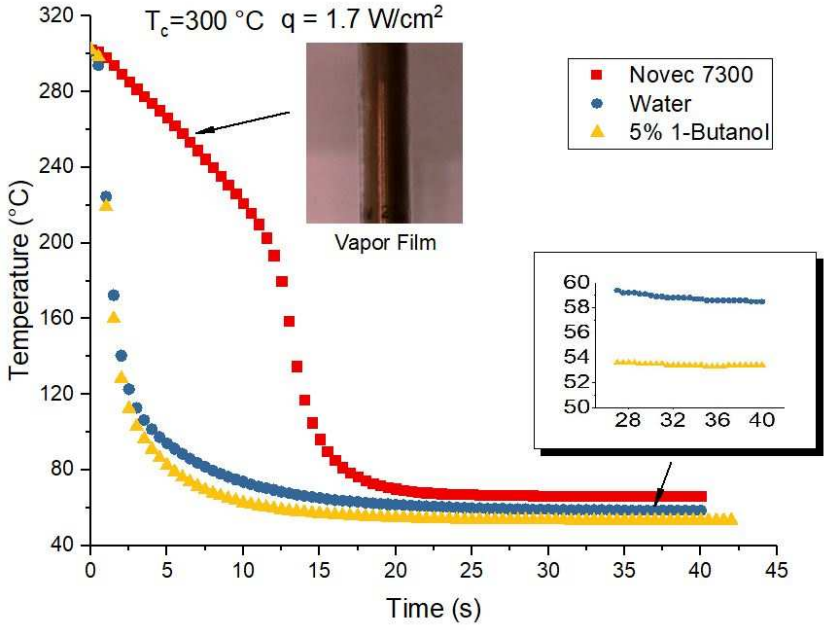
T$_c$=300 °C q = 1.7 W/cm^2
Novec 7300
Water
5% 1-Butanol
Vapor Film
Temperature (°C)
Time (s)

(c)

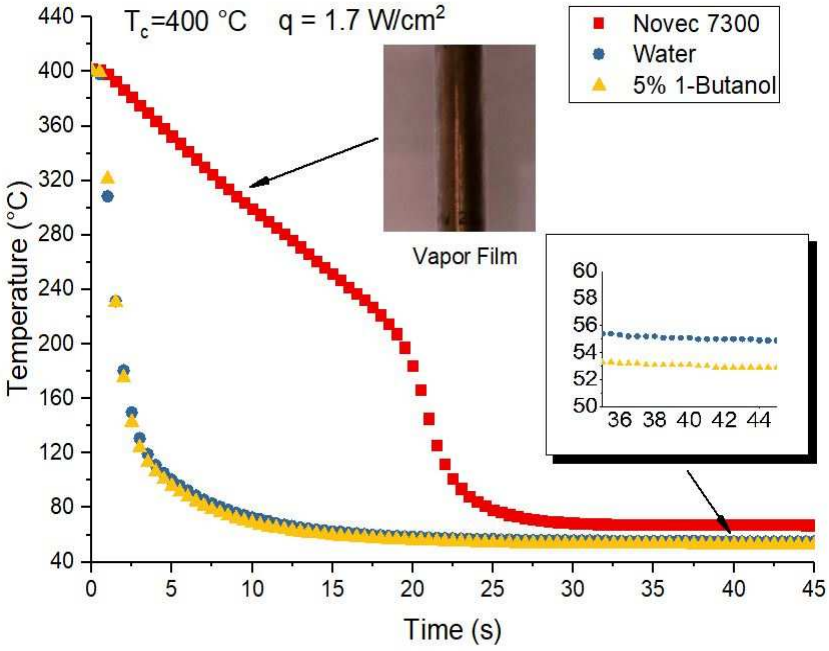
T$_c$=400 °C q = 1.7 W/cm^2
Novec 7300
Water
5% 1-Butanol
Vapor Film
Temperature (°C)
Time (s)

(d)

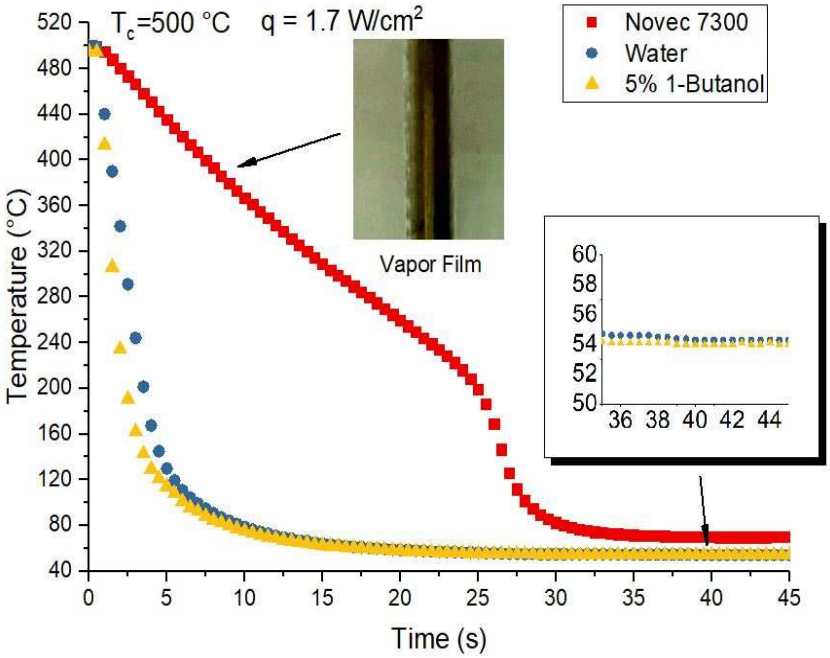
T$_c$=500 °C q = 1.7 W/cm^2
Novec 7300
Water
5% 1-Butanol
Vapor Film
Temperature (°C)
Time (s)

(e)

Figure 7 Heater surface temperature evolutions with different initial temperature of (a) 100 °C (b) 200 °C (c) 300 °C (d) 400 °C (e) 500 °C as a function of time after immersion in three solutions.

Heat is dissipated from heater surface to environment by convection q_{cv}, and radiation q_r. The total heat flux q_{tot} is constituted by these two parts as follow:

$$q_{tot} = q_{cv} + q_r \tag{2}$$

with

$$q_{cv} = h_{cv}(T_c - T_{env}) \tag{3}$$

and

$$q_r = \varepsilon\sigma T_c^4 \tag{4}$$

where h_{cv} is heat transfer coefficient of convection, ε is emissivity of heater surface, σ is Stefan-Boltzmann constant.

For heat flux of 1.7 W/cm^2, heater is at temperature of 500 °C before plunged in cooling liquid, the total heat flux dissipated by radiation can be calculated by Equation 4 and the result is 0.0767 W/cm^2 which is only 4.5% of total heat flux. Therefore the principal heat transfer is convection at testing temperature range.

The thickness of vapor film of Novec 7300 is insignificant by comparing with the diameter of heating cartridge. And the thermal conductivity of Novec 7300 vapor is much less than that of its liquid phase. Thus vapor film can be considered as thermal

insulation and heat transfer mode from solid-vapor interface to vapor-liquid interface is thermal conduction. The heat travels through vapor film can be expressed as follows:

$$UI + C(-\frac{dT_c}{dt}) = qA = -\frac{k}{e}A(T_c - T_{sat}) \quad (5)$$

where U and I are voltage and current applied on heating cartridge, k is thermal conductivity of Novec 7300 vapor, e is thickness of vapor film, T_{sat} is saturation temperature of Novec 7300.

For simplification, superheat of vapor is neglected and temperature at vapor-liquid interface is equal to saturation temperature when vapor film exists. According to recorded video, thickness of Novec 7300 vapor film displays a positive linear relationship with temperature difference T_c - T_{sat}. Therefore, the right part of Equation 5 is equal to a constant and then the heat transferred by vapor film is constant. The left part of Equation 5 can be converted as:

$$\frac{dT_c}{dt} = -\frac{qA-UI}{C} \quad (6)$$

Heating cartridge temperature decreases linearly with time, which is consistent with observation in Figure 7.

According to Equation 3, heat transfer coefficient of thermal convection can be calculated by following equation:

$$h_{cv} = \frac{q}{(T_{st}-T_l)} \quad (7)$$

where q is heat flux supplied by power supply, which is equal to UI/A, T_{st} is stabilized temperature of heater in liquid, T_l is liquid temperature. The calculation results for three solutions are presented in Figure 8. For all cases, heat transfer between heater and cooling liquid are strengthened with increase of heat flux. In 5% 1-butanol binary solution, heat transfer coefficient is the highest while the lowest in Novec 7300 for this range of heating power. The disparity between heat transfer coefficient in water and in 5% 1-butanol binary solution is enlarged with increase of heating power. It is because from around 50 °C, reversed Marangoni flow becomes effective which intensifies thermal convection and then improves heat transfer. However, the difference of heat transfer coefficient between in Novec 7300 and in 5% 1-butanol binary solution reduces with increase of heat flux. According to recorded videos, at heat flux of 1.16 W/cm^2 it is the incipience of nucleate boiling for Novec 7300 and the number of nucleation sites augments with increasing heating power. While for 5% 1-butanol binary solution and water, convection is the only heat transfer mode during this heat flux range. As a consequence, heat transfer mode changes from monophasic to diphasic in Novec 7300, which significantly enhances heat dissipation by vaporization.

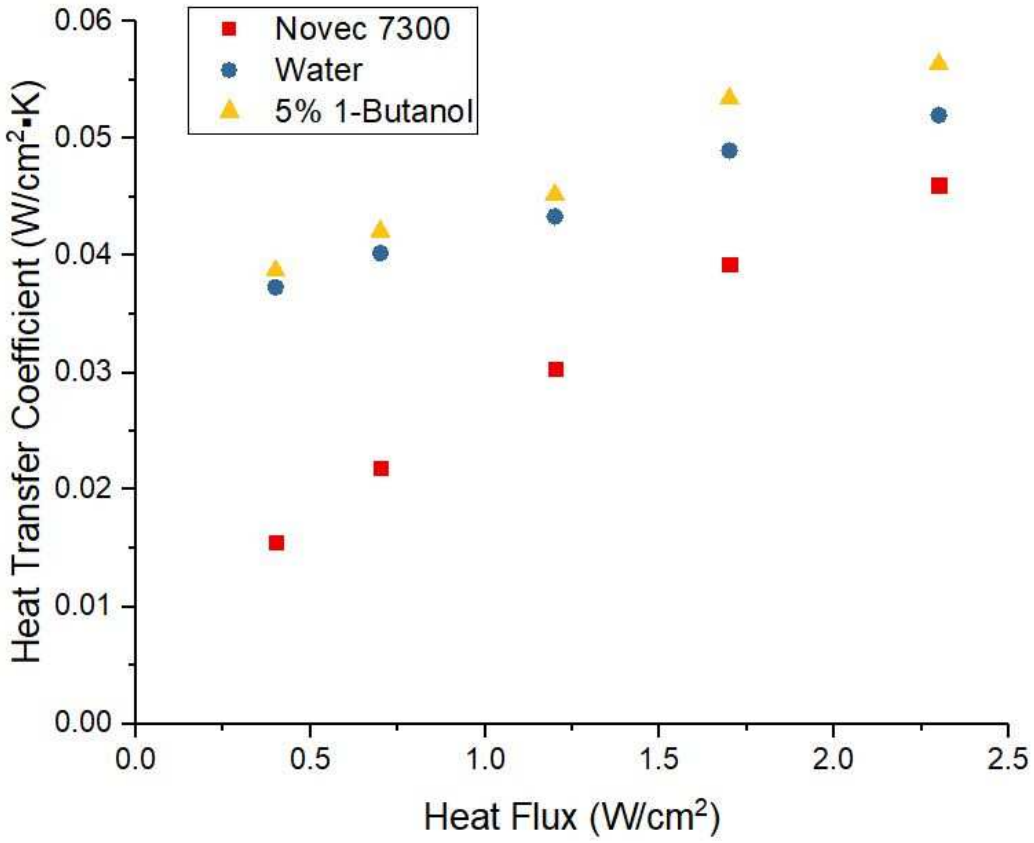

Figure 8 Evolution of heat transfer coefficient as a function of heat flux for three solutions.

3.2 Immersion cooling

First of all, the test of bare heater in three solutions was continued with higher heating power (0.41 ~ 25 W/cm^2). The heating processes were recorded by microscopic camera. For water, a couple of bubbles appear on heater surface from heat flux of 8.3 W/cm^2 and according to thermocouple measurement, heater temperature approaches the boiling point. With further heating, the fully developed nucleate boiling begins with heat flux of 14 W/cm^2. However for Novec 7300, the natural convection ends very early at heat flux of 0.72 W/cm^2 due to high volatility and low latent heat of vaporization.

Correspondingly the fully developed nucleate boiling starts early with heat flux of 5.5 W/cm^2. At maximum heat flux of 25 W/cm^2, the abrupt increase of heater temperature and observation of vapor film on heater surface demonstrate that film boiling occurs and critical heat flux attains. The coalescence of vapor bubbles on heater surface largely increases thermal resistance and surface temperature, and then considerably lower heat transfer coefficient, which is necessary to be avoided in immersion cooling. On the contrary, no bubble can be observed on heater surface when immersed in 5% 1-butanol binary solution with heat flux from 0.41 W/cm^2 to maximum of 25 W/cm^2. Although the boiling point of 1-butanol (117.7 °C) is a little higher than water (100 °C) and the saturated pressure of 1-butanol (0.93 kPa) is much lower than water (2.65 kPa), heater temperature reaches about 177 °C in 5% 1-butanol binary solution at maximum heat flux which largely exceeds the boiling point of both liquids. Moreover the pressure above liquid level stays at atmosphere pressure for each test. The addition of only 5% 1-butano cannot significantly change physical and thermodynamic properties of binary solution. Therefore the only supposed reason is the inversed thermal Marangoni flow. For common liquids (water and Novec 7300), heat is dissipated via fluid advection and thermal conduction. The main direction of fluid advection is upward driven by buoyancy force. The horizontal radial heat transfer mostly depends on thermal conduction. As a result, there is a substantial temperature gradient from heater surface outwardly to liquid bulk and along heater surface. With proper heat flux, liquid near heater surface will be heated up to exceed saturation temperature and then vaporized to form bubbles. That is why bubbles appear on heater surface when temperature dose not surpass boiling point

of liquid. For self-rewetting liquid, the thermal Marangoni effect is characterized by the thermal Marangoni number:

$$Ma_T = -\frac{\partial \gamma}{\partial T}\frac{L\Delta T_{int}}{\mu \alpha} \quad (8)$$

where γ is the interfacial tension, ΔT_{int} is the temperature difference across interface, L is the characteristic length, μ is the dynamic viscosity, and α is the thermal diffusivity. Thermal Marangoni effect is proportional to temperature gradient and the direction of inverse thermal Marangoni flow is from cold region to hot region. Because of buoyancy force, hotter liquid accumulate at heater upper end and then create temperature gradient along heater surface. Colder liquid is driven by thermal Marangoni effect from lower end of heater towards upper end along heater surface which accelerates fluid advection and eliminate hotter liquid near heater surface. Thermal Marangoni effect relies on temperature gradient on heater surface, thus the final result is that the temperature of liquid near heater surface is approximate homogenous and will not reach saturation temperature of 5% 1-butanol binary solution. Figure 9 shows the heat transfer phenomena of each testing solution at maximum heat flux of 25 W/cm^2.

Water - 25 W/cm^2 5% 1-Butanol – 25 W/cm^2 Novec 7300 – 25 W/cm^2

Figure 9 Screenshots of heater immersed in three solutions with heat flux of 25 W/cm^2.

With built-in thermocouple in heater and additional thermocouple in liquid far enough away from heater, the calculation of temperature difference ΔT between heater and environmental liquid is based on thermocouple measurements. Lower temperature difference means better cooling effect. Figure 10 represents temperature difference evolution in three testing liquid during incremental heating. Power input equipment was controlled by adjusting voltage. Voltage was increased by step of 20 V from 70 V to 230 V. Accordingly, heat flux increases from 2.3 W/cm^2 to 25 W/cm^2. At the beginning of heating, temperature difference in 5% 1-butanol binary solution is the lowest while much higher in Novec 7300 with relative low heating power. But when increasing heating power, the situation is totally reversed. Temperature difference becomes lowest in Novec 7300 while highest in 5% 1-butanol binary solution. For Novec 7300, an abnormal rise of temperature difference at the highest heating power indicates the occurrence of critical heat flux, which is in consistent with the observation of recorded videos. At lower heating power, sudden drop of temperature difference can be observed when increasing heat load. It is because that Novec 7300 possesses low heat capacity and heat transfer coefficient, sudden increase of heat flux cannot be dissipated at first time and then heater is heated up more than normal level. After a very short time, intensified convection takes away superheated liquid near heater surface and temperature difference drops. Heat transfer returns to equilibrium state. By further increasing heating power, the incipience of fully developed nucleate boiling largely improves heat transfer performance. Therefore the effect of thermal impact is weakened until its disappearance. For water, temperature difference development is moderate due

to high heat capacity. However, temperature difference suffers similar decrease in 5% 1-butnaol binary solution after increasing heat load at higher heating power. But the explainable reason is supposed to be different. Because of same high heat capacity, temperature difference evolution is mild at lower heating power. However at higher heating power, temperature gradient on heater surface is so strong that considerable Marangoni flow is created to strengthen convection and further lower heater surface temperature after increasing heat load. Temperature difference drops more gently in 5% 1-butanol binary solution instead of abrupt decrease in Novec 7300. By comparing fully developed nucleate boiling performance, Novec 7300 shows lower temperature difference than water. With same heat flux, nucleate boiling in Novec 7300 is more violent than in water (Figure 9), which intensifies thermal convection near heater surface and then improves heat transfer.

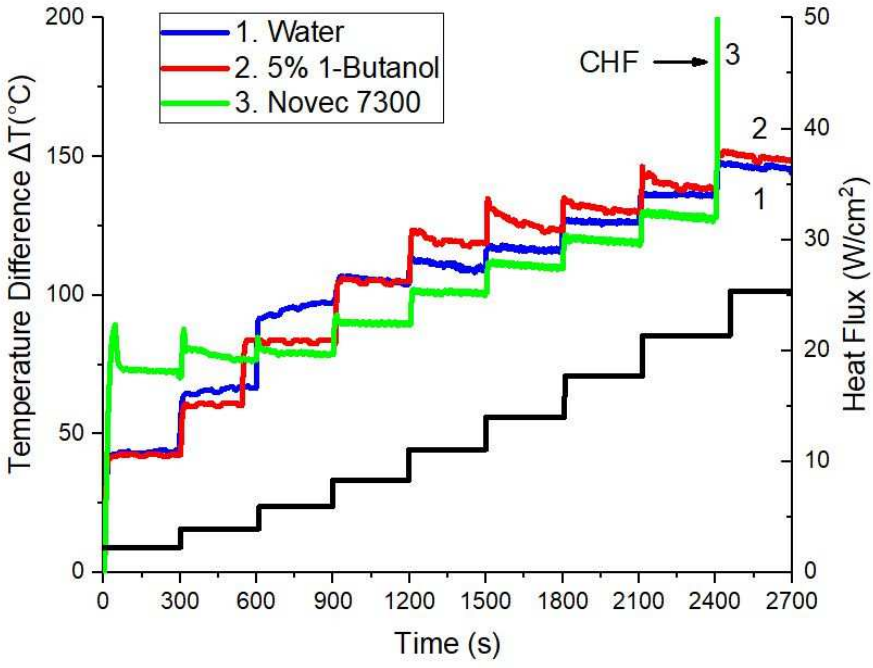

Figure 10 Heater temperature evolutions in three solutions under different heating power.

By referring to heat transfer coefficient (Figure 11), analogous results are obtained. Heat transfer coefficient is the highest in 5% 1-butanol solution at lower heating power while the highest in Novec 7300 with higher heat flux. In figure 11, the results of heat transfer coefficient in section 1 are also included. Heat transfer coefficient in Novec 7300 surpasses other liquids at heat flux of 5.5 W/cm^2. According to above discussion, it is exactly the incipience of fully developed nucleate boiling. Similarly, heat transfer coefficient in water exceeds that in 5% 1-butanol binary solution from the moment when nucleate boiling becomes fully developed. Overall, the change of heat transfer mode from monophasic to diphasic can significantly improve cooling performance.

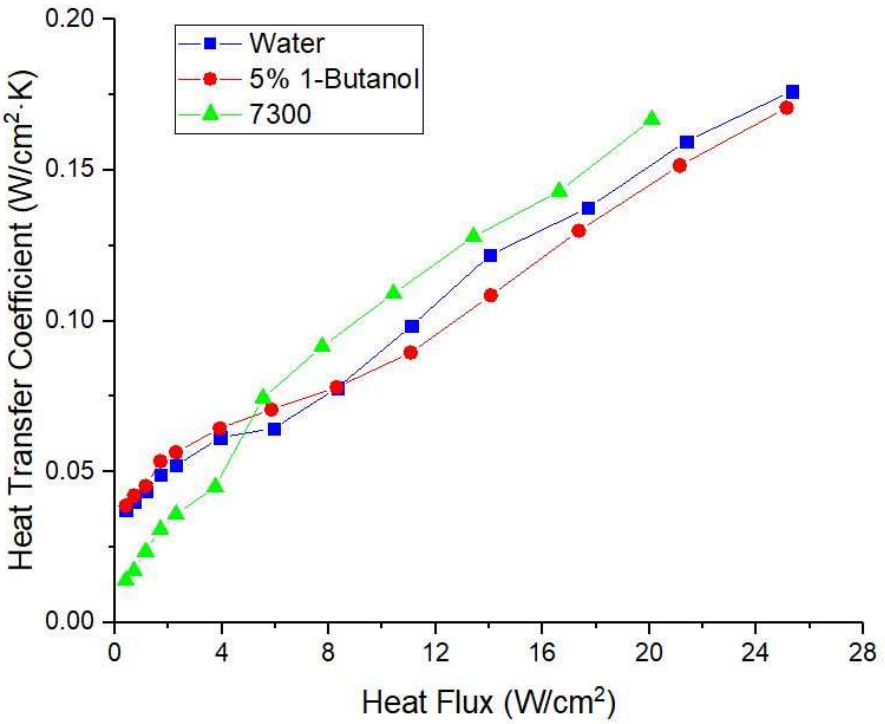

Figure 11 Evolution of heat transfer coefficient as a function of heat flux for three solutions from 0.41 W/cm^2 to 25 W/cm^2.

Figure 12 compares cooling performance between bare heater and heater with porous shell P1 in three testing solutions. For investigation of cooling performance in water, temperature difference of P1 is lower than bare heater at low heat flux due to increased heat exchange area and high effective thermal conductivity. But this improvement decreases with augmentation of heating power. Even at maximum heat flux of 25 W/cm^2, film boiling occurs and critical heat flux attains. Unlike temperature difference investigation, heat transfer coefficient evolution shows opposite trend. Heat transfer coefficient of bare heater demonstrates higher than that of P1 at high heat flux and lower at low heating power. The turning point coincides with heat flux of 8.3 W/cm^2, from which nucleate boiling begins. The recorded videos can give some clues to explain the deterioration of heat transfer coefficient at high heating power. Unlike intense growth and departure of bubbles from heater surface in water, few bubbles can escape through porous structure of P1. Vaporized bubbles are trapped in cavity and have difficulty to penetrate narrow pores by buoyancy force. Moreover liquid capillary effect impedes separation of bubbles. When vapor is generated on heater surface, buoyancy force drives bubbles upward and outward to separate out. But with porous shell, capillary pressure drives liquid towards heat surface via porous structure, which obstructs the outward departure path of bubbles. Accumulated bubbles on heater surface leads to increase of thermal resistance and then deterioration of heat transfer. For the case of 5% 1-butanol binary solution, the heat transfer coefficient of P1 is always higher than heater. The same as mentioned above, no indication of nucleate boiling can be found for P1 and

heater. With porous shell P1, temperature gradient lies not only on heater surface but also through pores. Therefore, thermal Marangoni flow runs simultaneously from lower end to upper end on heater surface and through porous structure. Moreover capillary effect assists liquid penetrates through pores. Intensified liquid convection near heater surface improves cooling effect and this improvement enhances with increase of temperature gradient as well as heating power. With addition of radially inward thermal Marangoni flow, porous shell P1 improves heat transfer when compared with the case of bare heater. Concerning heat transfer performance in Novec 7300, critical heat flux attains at 8.1 W/cm^2 and 25 W/cm^2 for P1 and bare heater respectively. Heat transfer coefficient of P1 is obviously lower than bare heater at heat flux of 5.7 W/cm^2 when fully developed nucleate boiling starts. The reason is the same as for water case. Trapped vapor bubbles increase thermal resistance and deteriorate heat transfer. Heat flux when film boiling occurs for P1 in Novec 7300 is lower than that in water. High volatility and low vaporization latent heat of Novec 7300 which cause liquid more easily to vaporize to become vapor. As a result, more Novec 7300 vapor bubbles accumulate on heater surface with lower heat flux by comparing to the case in water.

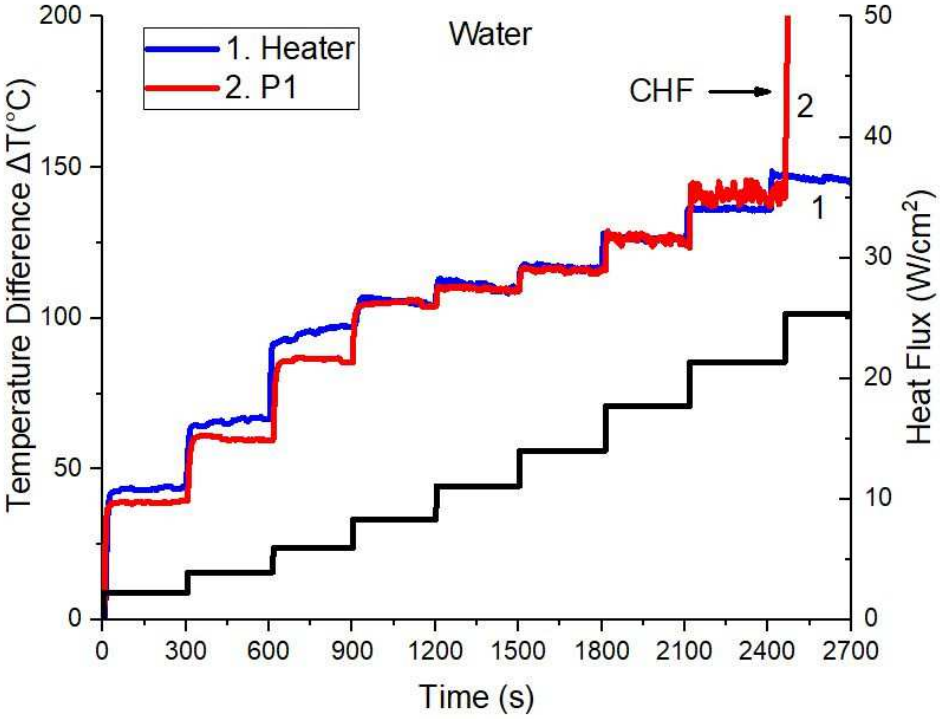
Water
1. Heater
2. P1
CHF
2
1
Temperature Difference ΔT(°C)
Heat Flux (W/cm²)
Time (s)
0
50
100
150
200
0
10
20
30
40
50
0
300
600
900
1200
1500
1800
2100
2400
2700

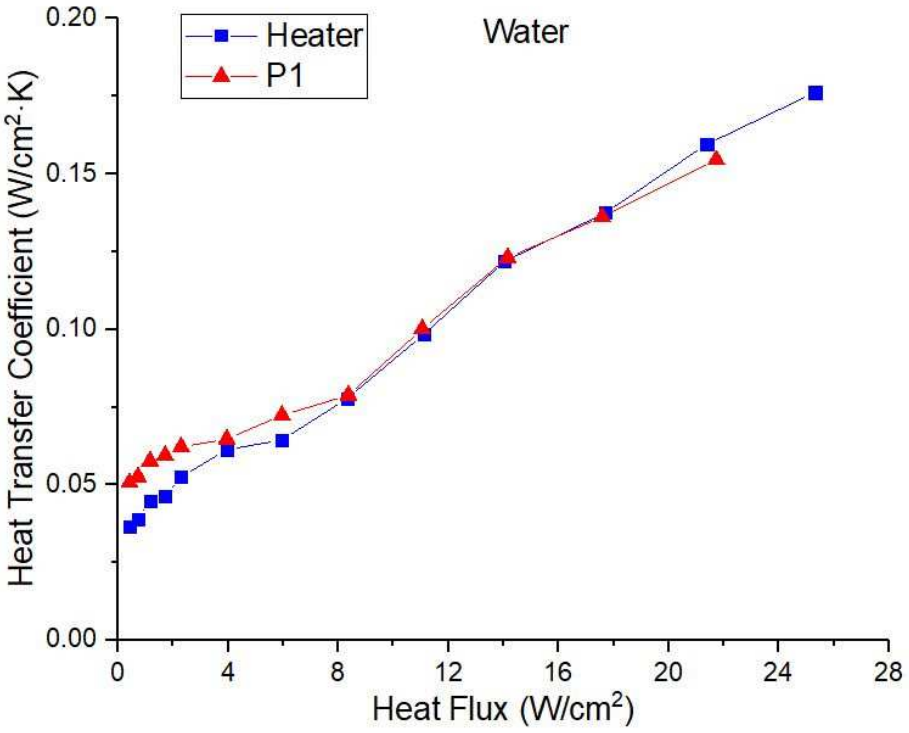
Water
Heater
P1
Heat Transfer Coefficient (W/cm²·K)
Heat Flux (W/cm²)
0.00
0.05
0.10
0.15
0.20
0
4
8
12
16
20
24
28

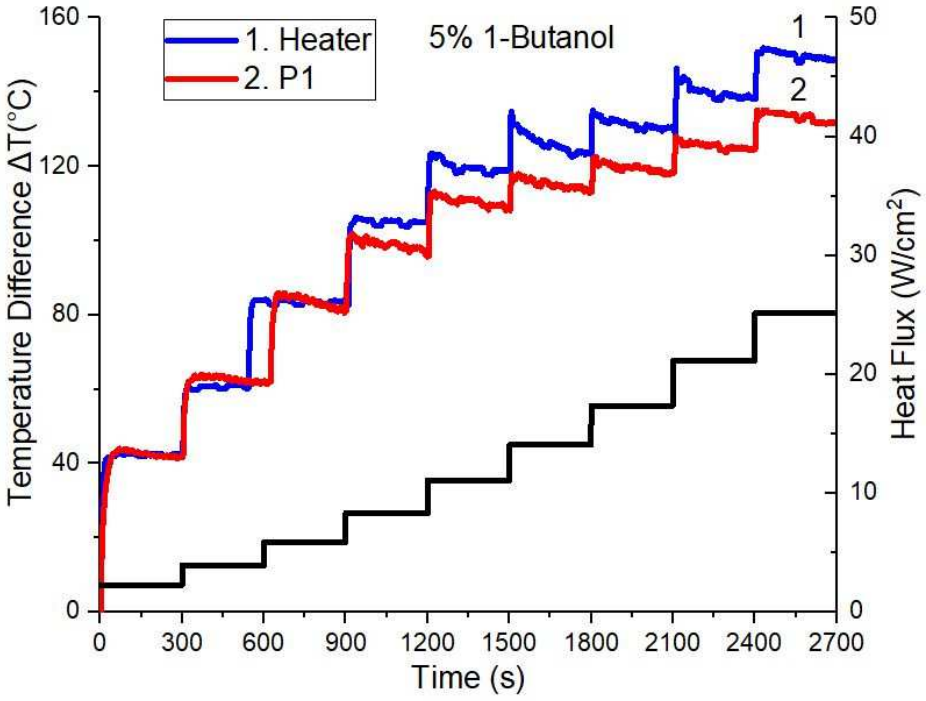
1. Heater
2. P1
5% 1-Butanol
1
2
Temperature Difference ΔT(°C)
Heat Flux (W/cm²)
Time (s)
0
40
80
120
160
0
10
20
30
40
50
0
300
600
900
1200
1500
1800
2100
2400
2700

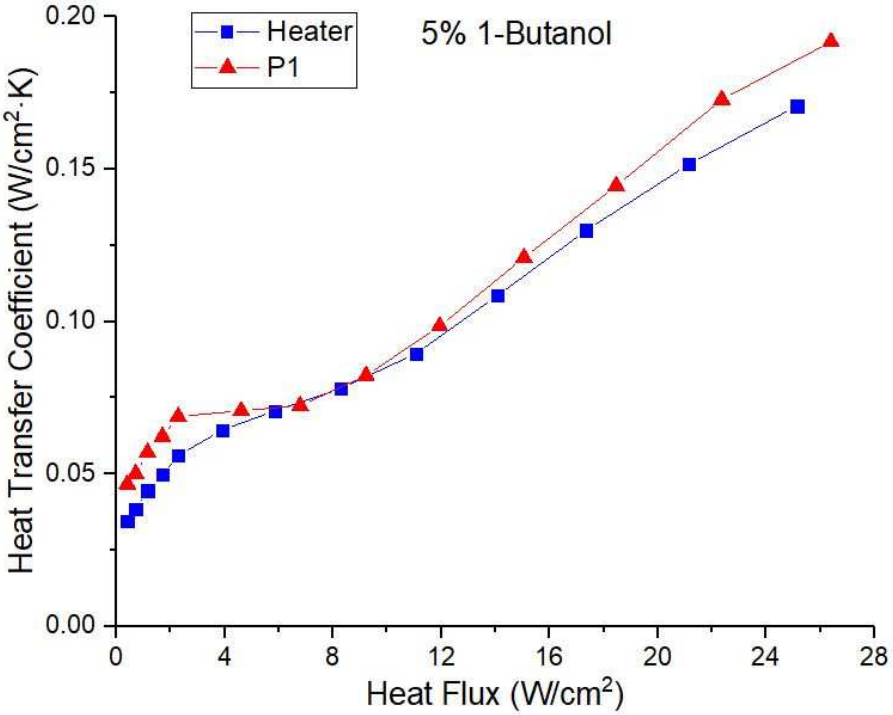
Heater
P1
5% 1-Butanol
Heat Transfer Coefficient (W/cm²·K)
Heat Flux (W/cm²)
0.00
0.05
0.10
0.15
0.20
0
4
8
12
16
20
24
28

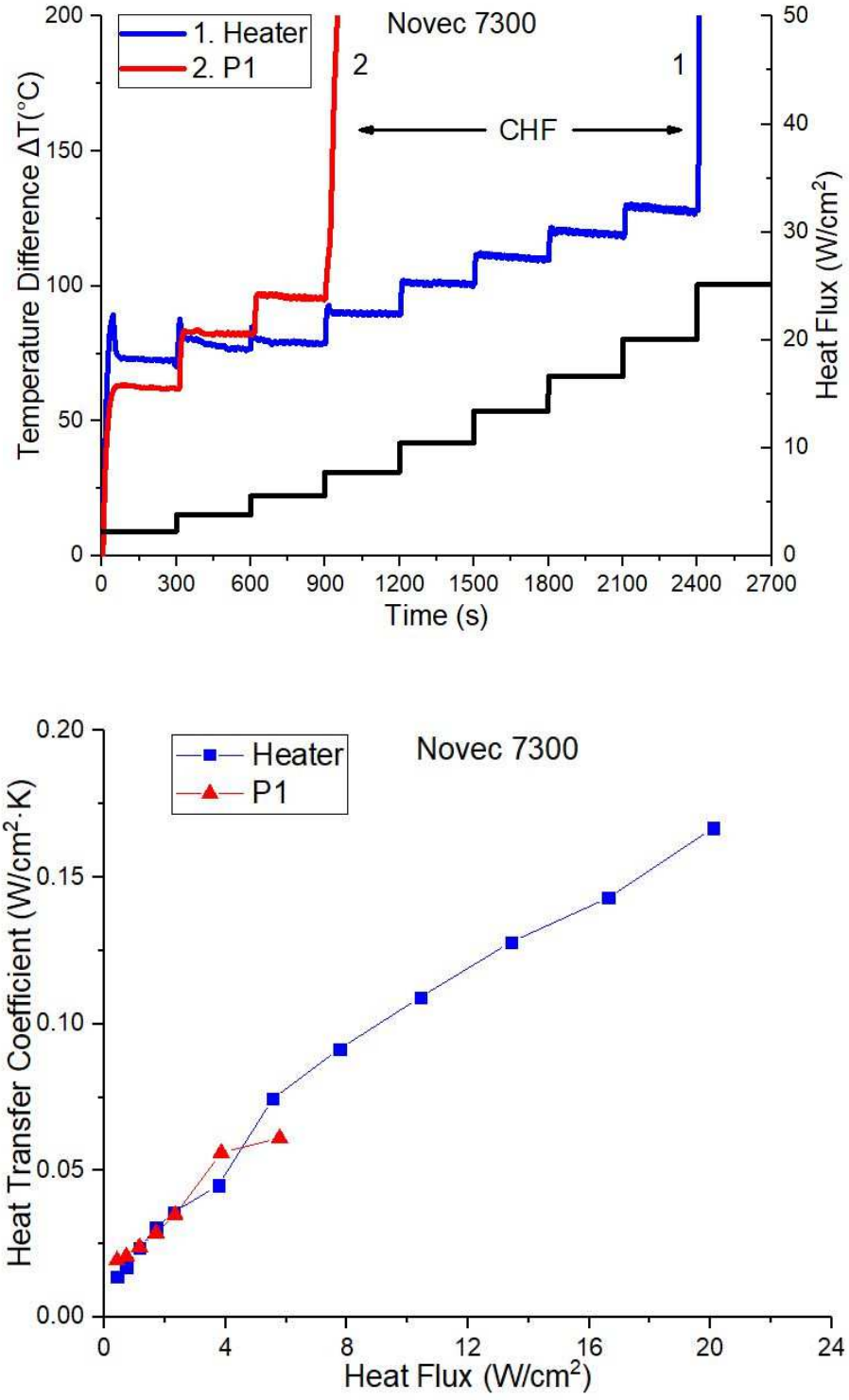

Figure 12 Effect of porous materiel on immersion cooling in three solutions.

Figure 13 represents effect of three different metal shells (P0, P1, and P2) on immersion cooling in three liquids (water, 5% 1-butanol binary solution, Novec 7300). When immersed in water, heater with metal shells shows similar cooling performance for P0 and P1 at low heating power. The case of P2 displays lower heat transfer coefficient because of lower effective thermal conductivity. With increase of heat flux, thermal conduction is no longer dominant in heat transfer. There is a large disparity of heat transfer performance between porous shell and flat shell. The case of P0 shows much higher temperature difference and much lower heat transfer coefficient than P1 and P2 despite of high effective thermal conductivity. The supposed reason is that the contact between heater and P0 is not perfect. Residual air in gap possess very low thermal conductivity, so the total thermal resistance from heater surface to liquid is increased according to equation $R_{tot} = \frac{R_{air}R_s}{R_{air}+R_s}$, where R_{air} and R_s is thermal resistance of air and flat shell P0 respectively. At high heating power, for case of P1 and P2, heater surface contacts with liquid directly and heat is dissipated via conduction, convection and phase change. However for P0, heat is dissipated through air, which situates between heater and brass shell, almost only by conduction. Thus heater temperature is significantly augmented at high heat flux. With respect to comparison between porous materials, P1 shows slightly better heat transfer than P2. Capillary pressure Δp in porous structure can be calculated by Young–Laplace equation:

$$\Delta p = \frac{2\gamma \cos\theta}{a} \tag{9}$$

where θ is contact angle between liquid and porous structure, a is pore diameter. Both P1 and P2 are made of copper foam, so contact angle is the same. Average pore diameter

of P1 is lower than P2. Consequently capillary pressure in P1 is higher than P2, which induces faster liquid flow through porous structure thereby strengthens heat transfer. However, bubbles are easier to escape from P2 due to larger average pore diameter. So there is no incident of film boiling for heater with P2 at maximal heat flux. Regarding immersion cooling in 5% 1-butanol binary solution, heater with porous shells demonstrates improved cooling effect. P1, whose porosity is smaller, proves lower temperature difference and higher heat transfer coefficient than P2. Moreover, at heat flux of 14.2 W/cm2, the increase of heat transfer coefficient with P1 compared to P2 is higher in 5% 1-butanol binary solution (12.2%) than in water (8.5%). The increased capillary pressure cannot completely explain this phenomenon. One of influencing factor is supposed to be the characteristic length for Marangoni effect. Porous structure looks like a channel with holes. The effective characteristic length should be calculated by channel length subtract length where holes situate. Therefore higher porosity means lower effective characteristic length. In the light of equation 8, P1 induces more intense thermal Marangoni flow than P2, which improves heat dissipation as mentioned above. Owing to vapor trapped in pores, film boiling appears at heat flux of 8.1 W/cm^2 and 18.1 W/cm^2 for P1 and P2 separately when immersed in Novec 7300. Porosity of P2 is higher than P1, thus generated bubbles are easier to escape and critical heat flux arrives at higher value for the case with P2. Heat transfer coefficient of P0 is much lower than porous shells and this difference increases with rise of heating power as in water and 5% 1-butanol binary solution.

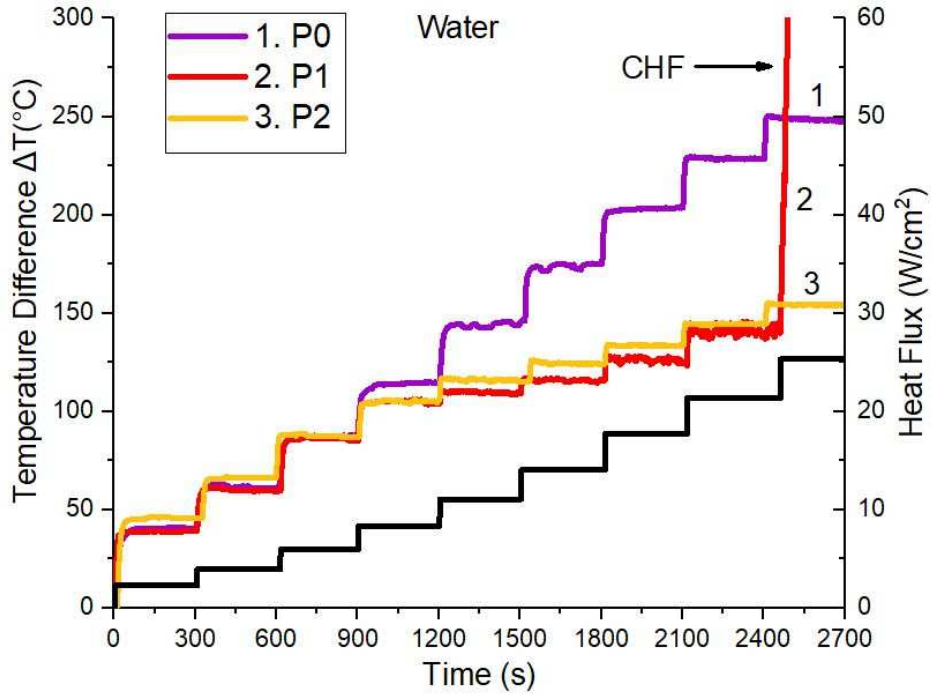
Water
1. P0
2. P1
3. P2
CHF
1
2
3
Temperature Difference ΔT(°C)
Heat Flux (W/cm²)
Time (s)
0
300
600
900
1200
1500
1800
2100
2400
2700
0
50
100
150
200
250
300
0
10
20
30
40
50
60

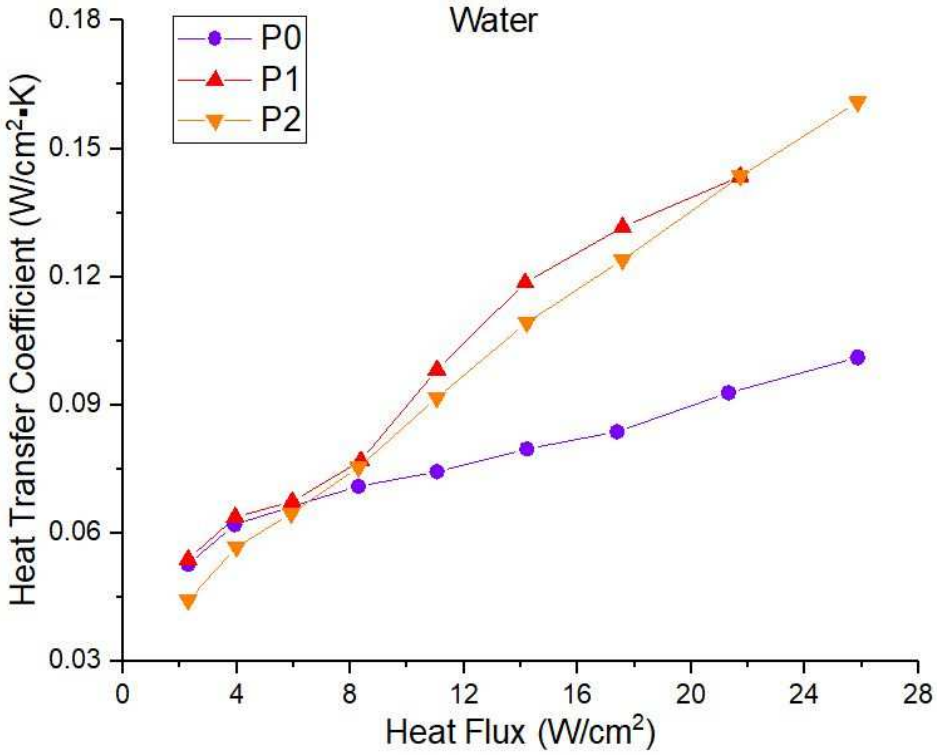
Water
P0
P1
P2
Heat Transfer Coefficient (W/cm²·K)
Heat Flux (W/cm²)
0
4
8
12
16
20
24
28
0.03
0.06
0.09
0.12
0.15
0.18

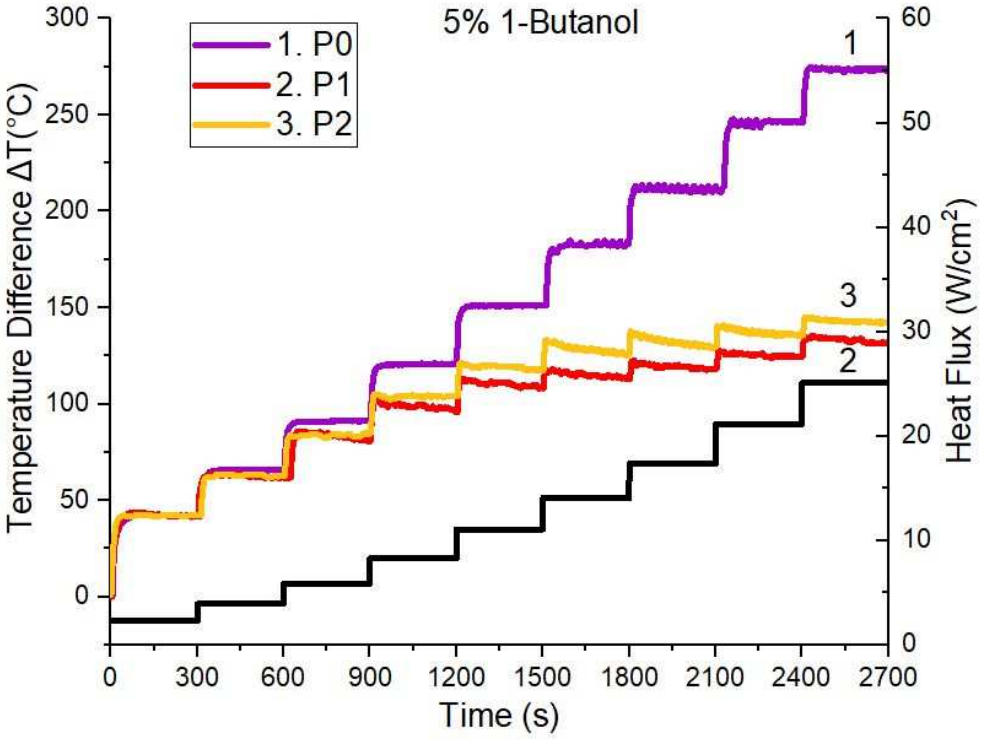
5% 1-Butanol
1. P0
2. P1
3. P2
Temperature Difference ΔT(°C)
Heat Flux (W/cm²)
Time (s)
1
2
3
0
50
100
150
200
250
300
0
10
20
30
40
50
60
0
300
600
900
1200
1500
1800
2100
2400
2700

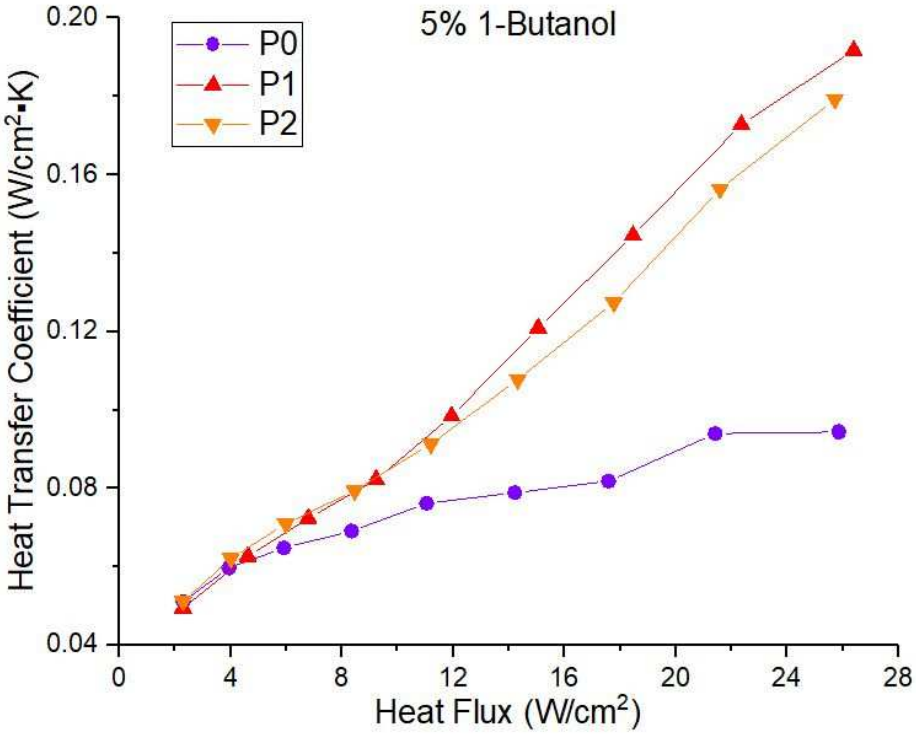
5% 1-Butanol
P0
P1
P2
Heat Transfer Coefficient (W/cm²•K)
Heat Flux (W/cm²)
0.04
0.08
0.12
0.16
0.20
0
4
8
12
16
20
24
28

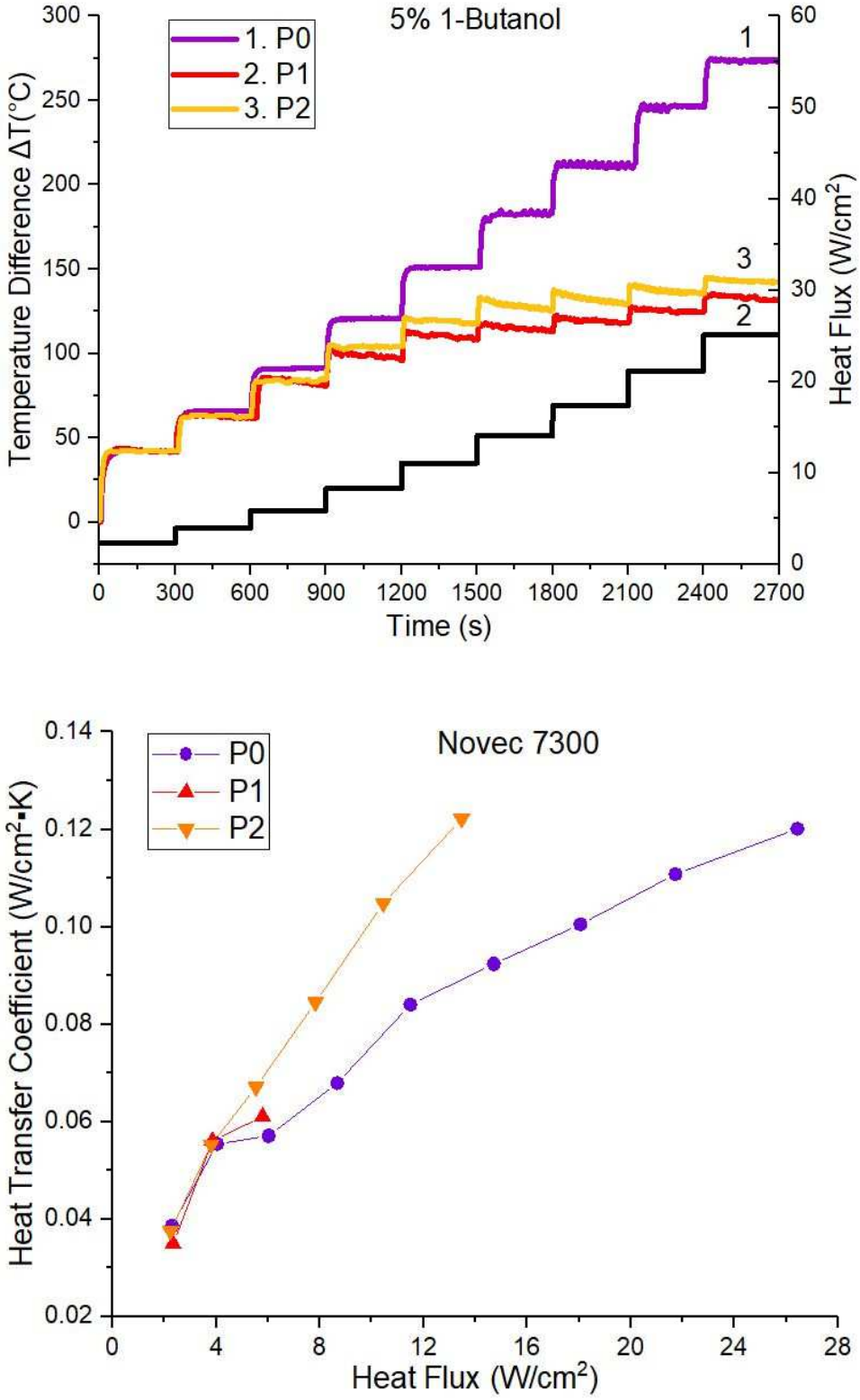

Figure 13 Effect of metal shell porosity on immersion cooling in three solutions.

Last, an overall comparison among combinations of four heater states (bare, P0, P1, P2) and three cooling liquids (water, 5% 1-butanol binary solution, Novec 7300) was made in order to find optimal combination. The results are presented in Figure 14 and divided in four stages. At weak heat flux, naturel convection is dominant in heat transfer. Thus heater with P1 immersed in water shows highest heat transfer coefficient. With increase of heating power, inverse thermal Marangoni flow helps heater with P1 to have the best cooling effect in 5% 1-butanol binary solution when heater surface temperature surpasses 50 °C. From heat flux of 5.5 W/cm^2, bare heater in Novec 7300, thanks to fully developed nucleate boiling, demonstrates outstanding heat transfer performance until the occurrence of film boiling. At as much as 25 W/cm2, most combination attains the critical heat flux. However heat transfer mode of heater with P1 in 5% 1-butanol binary solution is still naturel convection. And then this combination becomes the best choice for immersion cooling at this considerably high heat flux.

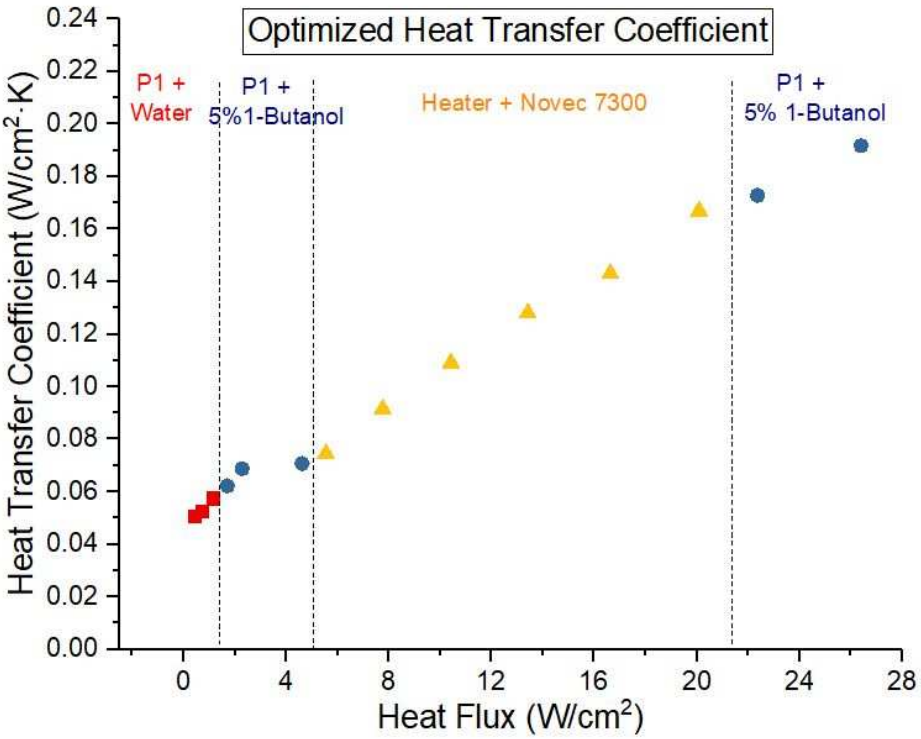

Figure 14 Optimized evolution of heat transfer coefficient as function of heat flux.

4. Conclusions

In this study, rapid cooling of heating cartridge in three solutions (water, 5% 1-butanol binary solution, Novec 7300) and immersion cooling of heater without or with metal shells of different porosity (P0, P1, P2) have been experimentally investigated. Thermal performance results and conclusions are presented as follows:

1. For rapid cooling, heater in 5% 1-butanol binary solution showed highest temperature reduction rate and lowest stabilized temperature in liquid owing to accelerated bubbles separation by inverse thermal Marangoni flow. Vapor film appeared on heater surface in Novec 7300 when surface temperature exceeds 200 °C, which led to

gentle temperature decrease. Thickness of vapor film depended on surface temperature while it was independent of heat flux.

2. For immersion cooling in testing liquid with increasing heat flux, different combination of heater and liquid revealed different cooling performance according to power input. At low heat flux, heater immersed in water with porous shell P1 displayed the best heat transfer. From 1.7 W/cm^2, assistance of inverse thermal Marangoni effect made heater with P1 in 5% 1- butanol binary solution to show the highest heat transfer coefficient. During a large range of heat flux from 5.5 W/cm^2 to 20.1 W/cm^2, bare heater in Novec 7300 demonstrated the best cooling effect thanks to violent nucleate boiling. At maximum heat flux, heater with P1 in 5% 1-butanol binary solution was the best choice for immersion cooling without vapor bubbles generation.
3. Inverse Marangoni effect can enhance heat transfer only in domain of naturel convection. Similarly capillary effect by porous materiel played a part before occurrence of nucleate boiling. Liquid of high volatility and low boiling point, like Novec 7300, was suitable for most heat dissipation application owing to violent nucleate boiling at relative low heat flux. Thermal phenomenon in 5% 1-butanol binary solution was interesting that no phase change phenomenon can be found even at heat flux of 26.4 W/cm^2. The combination of porous surface and immersion in 5% 1-butanol binary solution had a potential application for cooling of certain sensitive electronic components.

Corresponding Author

*E-mail: maximilien0809@hotmail.com

Tel: +33 (0)32 27 51 19 60

Address: LAMIH Laboratory, Polytechnic University of Hauts-de-France, Gromaire building, Le Mont Houy, F59313 Valenciennes CEDEX 9, France

Acknowledgements

This work has been achieved within the framework of CE2I project (Convertisseur d'Énergie Intégré Intelligent). CE2I is co-financed by European Union with the financial support of European Regional Development Fund (ERDF), French State and the French Region of Hauts-de-France. The authors also would like to acknowledge 3M France for providing dielectric liquid.

References

[1] M. Arik, A. Bar-Cohen, Immersion cooling of high heat flux microelectronics with dielectric liquids, 4th International Symposium on Advanced Packaging Materials Processes, Properties and Interfaces, IEEE, Braselton, GA, 1998, pp. 229-247.

[2] M. Arik, A. Bar-Cohen, Ebullient cooling of integrated circuits by Novec fluids, GE Global Research, Technical Report No. GRC027, 2002.

[3] K.N. Rainey, S.M. You, S. Lee, Effect of pressure, subcooling, and dissolved gas on pool boiling heat transfer from microporous surfaces in FC-72, Journal of Heat Transfer 125(1) (2003) 75-83.

[4] M.S. El-Genk, Immersion cooling nucleate boiling of high power computer chips, Energy conversion and management 53(1) (2012) 205-218.

[5] A. Bar-Cohen, G. Sherwood, M. Hodes, G. Solbreken, Gas-assisted evaporative cooling of high density electronic modules, IEEE Transactions on Components, Packaging, and Manufacturing Technology: Part A 18(3) (1995) 502-509.

[6] T.Y.T. Lee, Application of Dielectric Binary Mixtures in Electronic Cooling—Nucleate Pool Boiling Regime, Journal of Electronics Manufacturing 7(02) (1997) 93-103.

[7] M. Arik, A. Bar-Cohen, Pool boiling of perfluorocarbon mixtures on silicon surfaces, International Journal of Heat and Mass Transfer 53(23-24) (2010) 5596-5604.

[8] C. Marangoni, Sull'espansione delle goccie d'un liquido galleggianti sulla superfice di altro liquido (1865).

[9] R. Vochten, G. PETRE II, Experimental determination of the heat of reversible absorption of some alcohols, Journal of Colloid and Interface Science 42 (1973) 320-327.

[10] P. Chen, S. Harmand, S. Ouenzerfi, J. Schiffler, Marangoni flow induced evaporation enhancement on binary sessile drops, The Journal of Physical Chemistry B 121(23) (2017) 5824-5834.

[11] S. Zhou, L. Zhou, X. Du, Y. Yang, Heat transfer characteristics of evaporating thin liquid film in closed microcavity for self-rewetting binary fluid, International Journal of Heat and Mass Transfer 108 (2017) 136-145.

[12] S. Tsang, Z.H. Wu, C.H. Lin, C. Sun, On the evaporative spray cooling with a self-rewetting fluid: Chasing the heat, Applied Thermal Engineering 132 (2018) 196-208.

[13] Y. Hu, T. Liu, X. Li, S. Wang, Heat transfer enhancement of micro oscillating heat pipes with self-rewetting fluid, International Journal of Heat and Mass Transfer 70 (2014) 496-503.

[14] M. Zhu, J. Huang, M. Song, Y. Hu, Thermal performance of a thin flat heat pipe with grooved porous structure, Applied Thermal Engineering (2020) 115215.

[15] R. Savino, C. Piccolo, R. Fortezza, Y. Abe, Heat pipes with self-rewetting fluids under low-gravity conditions, Microgravity Science and Technology 19(3-4) (2007) 75-77.

[16] A. Sitar, I. Golobic, Heat transfer enhancement of self-rewetting aqueous n-butanol solutions boiling in microchannels, International Journal of Heat and Mass Transfer 81 (2015) 198-206.

[17] Y. Hu, S. Chen, J. Huang, M. Song, Marangoni effect on pool boiling heat transfer enhancement of self-rewetting fluid, International Journal of Heat and Mass Transfer 127 (2018) 1263-1270.

[18] Y. Hu, H. Wang, M. Song, J. Huang, Marangoni effect on microbubbles emission boiling generation during pool boiling of self-rewetting fluid, International Journal of Heat and Mass Transfer, 134 (2019) 10-16.

[19] Y. Hu, S. Zhang, X. Li, S. Wang, Heat transfer enhancement of subcooled pool boiling with self-rewetting fluid, International Journal of Heat and Mass Transfer 83 (2015) 64-68.

[20] H. Sakashita, A. Ono, Y. Nakabayashi, Measurements of critical heat flux and liquid–vapor structure near the heating surface in pool boiling of 2-propanol/water mixtures, International Journal of Heat and Mass Transfer 53(7-8) (2010) 1554-1562.

[21] D. Zhong, J. Meng, Z. Li, Z. Guo, Critical heat flux for downward-facing saturated pool boiling on pin fin surfaces, International Journal of Heat and Mass Transfer 87 (2015) 201-211.

[22] J.W. Liu, D.J. Lee, A. Su, Boiling of methanol and HFE-7100 on heated surface covered with a layer of mesh, International Journal of Heat and Mass Transfer 44(1) (2001) 241-246.

[23] J. Xu, X. Ji, W. Zhang, G. Liu, Pool boiling heat transfer of ultra-light copper foam with open cells, International Journal of Multiphase Flow 34(11) (2008) 1008-1022.

[24] Y. Yang, X. Ji, J. Xu, Pool boiling heat transfer on copper foam covers with water as working fluid, International Journal of Thermal Sciences 49(7) (2010) 1227-1237.

[25] B.J. Jones, J.P. McHale, S.V. Garimella, The influence of surface roughness on nucleate pool boiling heat transfer, Journal of Heat Transfer 131(12) (2009) 121009.

[26] H. Honda, H. Takamatsu, J.J. Wei, Enhanced boiling heat transfer from silicon chips with micro-pin fins immersed in FC-72, Journal of Enhanced Heat Transfer 10(2) (2003).

[27] S.H. Kim, G.C. Lee, J.Y. Kang, K. Moriyama, M.H. Kim, H.S. Park, Boiling heat transfer and critical heat flux evaluation of the pool boiling on micro structured surface, International Journal of Heat and Mass Transfer 91 (2015) 1140-1147.

[28] J.Y. Chang, S.M. You, Enhanced boiling heat transfer from microporous surfaces: effects of a coating composition and method, International Journal of Heat and Mass Transfer 40(18) (1997) 4449-4460.

[29] K.G. Rajulu, R. Kumar, B. Mohanty, H.K. Varma, Enhancement of nucleate pool boiling heat transfer coefficient by reentrant cavity surfaces, Heat and mass transfer 41(2) (2004) 127-132.

[30] R. Furberg, B. Palm, Boiling heat transfer on a dendritic and micro-porous surface in R134a and FC-72, Applied Thermal Engineering 31(16) (2011) 3595-3603.

[31] M.S. El-Genk, A. Suszko, Effects of inclination angle and liquid subcooling on nucleate boiling on dimpled copper surfaces, International Journal of Heat and Mass Transfer 95 (2016) 650-661.

[32] M.S. El-Genk, J.L. Parker, Enhanced boiling of HFE-7100 dielectric liquid on porous graphite, Energy Conversion and Management 46(15-16) (2005) 2455-2481.

[33] S. Jun, S. Sinha-Ray, A.L. Yarin, Pool boiling on nano-textured surfaces, International Journal of Heat and Mass Transfer 62 (2013) 99-111.

[34] M. Dharmendra, S. Suresh, C.S. Kumar, Q. Yang, Pool boiling heat transfer enhancement using vertically aligned carbon nanotube coatings on a copper substrate, Applied Thermal Engineering 99 (2016) 61-71.

[35] Y. Tang, B. Tang, Q. Li, J. Qing, L. Lu, K. Chen, Pool-boiling enhancement by novel metallic nanoporous surface, Experimental Thermal and Fluid Science 44 (2013) 194-198.

[36] E. Forrest, E. Williamson, J. Buongiorno, L.W. Hu, M. Rubner, R. Cohen, Augmentation of nucleate boiling heat transfer and critical heat flux using nanoparticle thin-film coatings, International Journal of Heat and Mass Transfer 53(1-3) (2010) 58-67.

[37] S.D. Park, S.B. Moon, I.C. Bang, Effects of thickness of boiling-induced nanoparticle deposition on the saturation of critical heat flux enhancement, International Journal of Heat and Mass Transfer 78 (2014) 506-514.

[38] I. Mudawar, T.M. Anderson, Parametric investigation into the effects of pressure, subcooling, surface augmentation and choice of coolant on pool boiling in the design of cooling systems for high-power-density electronic chips, Journal of Electronic Packaging 112(4) (1990) 375-382.

[39] K.N. Rainey, S.M. You, Pool boiling heat transfer from plain and microporous, square pin-finned surfaces in saturated FC-72, Journal of Heat Transfer 122(3) (2000) 509-516.

[40] K.H. Chu, Y. Soo Joung, R. Enright, C.R. Buie, E.N. Wang, Hierarchically structured surfaces for boiling critical heat flux enhancement, Applied Physics Letters 102(15) (2013) 151602.

[41] Z. Yao, Y.W. Lu, S.G. Kandlikar, Fabrication of nanowires on orthogonal surfaces of microchannels and their effect on pool boiling, Journal of Micromechanics and Microengineering 22(11) (2012) 115005.

[42] H.T. Phan, N. Caney, P. Marty, S. Colasson, J. Gavillet, Surface wettability control by nanocoating: the effects on pool boiling heat transfer and nucleation mechanism，International Journal of Heat and Mass Transfer 52(23-24) (2009) 5459-5471.

[43] Product information, 3M™ Novec™ 7300 Engineered Fluid. https://multimedia.3m.com/mws/media/338713O/3m-novec-7300-engineered-fluid.pdf/, 2020 (accessed 20 May 2020).

[44] R.J. Moffat, Describing the uncertainties in experimental results, Experimental Thermal and Fluid Science 1(1) (1988) 3-17.

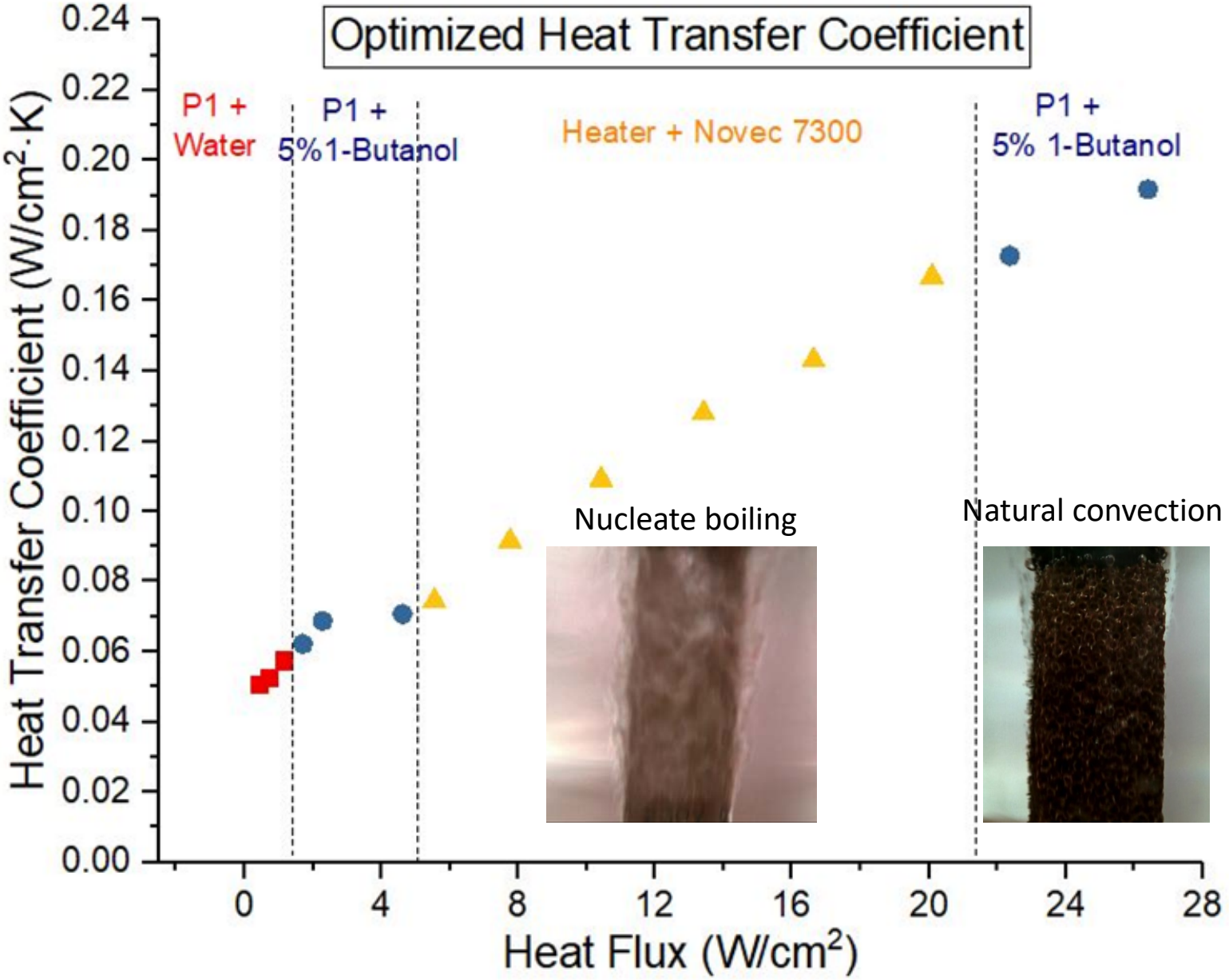
Optimized Heat Transfer Coefficient
P1 + Water
P1 + 5%1-Butanol
Heater + Novec 7300
P1 + 5% 1-Butanol
Nucleate boiling
Natural convection
Heat Transfer Coefficient (W/cm²·K)
Heat Flux (W/cm²)
0.00
0.02
0.04
0.06
0.08
0.10
0.12
0.14
0.16
0.18
0.20
0.22
0.24
0
4
8
12
16
20
24
28